

# STRUCTURAL RECORD OF VARISCAN THRUSTING AND SUBSEQUENT EXTENSIONAL COLLAPSE IN THE MICA SCHISTS FROM VICINITIES OF KAMIENIEC ZĄBKOWICKI, SUDETIC FORELAND, SW POLAND

Stanisław MAZUR & Dariusz JÓZEFIAK

*Instytut Nauk Geologicznych Uniwersytetu Wrocławskiego, 50-204 Wrocław pl. Maksa Borna 9*

Mazur, S. & Józefiak, D., 1999. Structural record of Variscan thrusting and subsequent extensional collapse in the mica schists from vicinities of Kamieniec Ząbkowicki, Sudetic foreland, SW Poland. *Ann. Soc. Geol. Polon.*, 69: 1–26.

**Abstract:** Two tectonic units of different metamorphic grade can be distinguished in the mica schists which crop out at the eastern margin of the Sudetic foreland near Kamieniec Ząbkowicki. The Kamieniec unit comprises mica schists containing garnet, staurolite and andalusite porphyroblasts, whereas the Byczeń unit is composed of mica schists having porphyroblasts of albite. The Byczeń unit is situated to the west of the Kamieniec unit in the north of the study area. The reverse order of the two units apparent in the south of that area results from displacement of their tectonic contact along a shallow WSW-dipping normal-slip shear zone cross-cutting earlier steeply dipping structures. Both the Kamieniec and Byczeń tectonic units are exposed on the inverted limb of a large SE-vergent synform, F<sub>2</sub>, as indicated by NW asymmetry of mesofolds and by gently inclined cleavage S<sub>2</sub> intersecting the steep foliation S<sub>1</sub>. The hinge zone of this fold is occupied by an orthogneiss body and the normal limb is represented by paragneiss of the Chałupki unit exposed further east.

The mica schists in the vicinities of Kamieniec Ząbkowicki have recorded three deformation events, D<sub>1</sub>, D<sub>2</sub> and D<sub>3</sub>. Deformation D<sub>1</sub> produced the main foliation S<sub>1</sub>, which, in the study area is now steeply NW-dipping. The locally preserved L<sub>1</sub> stretching lineation is trending, in general, E–W, although it is locally reoriented on the limbs of younger folds F<sub>2</sub>. The axes of the F<sub>2</sub> folds are oriented NE–SW and the accompanying penetrative axial cleavage S<sub>2</sub> show gentle dips to the W, SW or NW. The S<sub>2</sub> foliation is represented either by crenulation cleavage or, more frequently, by transposition foliation that has completely replaced the older foliation S<sub>1</sub>. Intersecting S<sub>2</sub> and S<sub>1</sub> surfaces define penetrative lineation L<sub>2</sub>, the most prominent linear structure in the area. Deformation D<sub>3</sub> was confined to low-angle normal-slip shear zones dipping to the SW. The S<sub>3</sub> foliation within the shear zones is parallel to S<sub>2</sub>, whereas the L<sub>3</sub> stretching lineation parallels the intersection lineation L<sub>2</sub>.

Kinematic indicators point to an E-directed overthrusting of the Byczeń unit by the Kamieniec unit during the D<sub>1</sub> event. The tectonic juxtaposition of both units resulted in metamorphic grade inversion. The subsequent deformation D<sub>2</sub> involved an irrotational shortening in the NW–SE direction, which produced the large-scale NE–SW-trending synform F<sub>2</sub>. Its western, inverted limb was subjected to an intense subvertical shortening. The progressive shortening was followed by development of normal-slip shallow-dipping shear zones D<sub>3</sub> showing top-to-SW or to-WSW sense of shear. The normal-slip shearing was related to SW-directed extensional collapse D<sub>3</sub> at the eastern margin of the Sudetic foreland.

**Key words:** mica schists, deformation, metamorphism, Sudetes, Variscan belt.

**Abstrakt:** W łupkach łyszczykowych okolic Kamieńca Ząbkowickiego wydzielamy dwie jednostki tektoniczne Kamieńca i Byczenia, różniące się stopniem metamorfizmu. Pierwsza z nich obejmuje łupki łyszczykowe z porfiroblastami granatu, staurolitu i andaluzytu, podczas gdy do drugiej należą łupki z porfiroblastami albitu. W skali całego metamorfiku Kamieńca Ząbkowickiego jednostka Byczenia występuje generalnie na zachód od jednostki Kamieńca, tak jak ma to miejsce w rejonie wsi Stolec. Odwrotne rozmieszczenie wychodni tych jednostek między Kamieńcem Ząbkowickim a Byczeniem jest efektem przemieszczenia na połogiej, zrzutowo-normalnej strefie ściśnania o upadzie ku WSW. Orientacja kliwa S<sub>2</sub> nachylonego mniej stromo niż foliacja S<sub>1</sub> oraz północno-zachodnia asymetria fałdów mezoskopowych dowodzą, że obie jednostki tektoniczne występują na krótszym skrzydle makrosyntagma obalonej ku SE. Dłuższemu skrzydłu synformy odpowiadają natomiast wychodnie paragnejsów wschodniej części metamorfiku Doboszowic (jednostka Chałupek).

W łupkach łyszczykowych z okolic Kamieńca Ząbkowickiego wyróżniliśmy trzy zespoły struktur deformacyjnych odpowiadające trzem etapom deformacji D<sub>1</sub>, D<sub>2</sub> i D<sub>3</sub> o zasięgu regionalnym. W etapie D<sub>1</sub> powstała foliacja S<sub>1</sub> zapadająca dziś w obszarze badań stromo ku NW oraz, zaznaczająca się tylko sporadycznie, lineacja z rozciągania L<sub>1</sub>. Generalny przebieg lineacji L<sub>1</sub> jest zbliżony do kierunku E–W, choć lokalnie uległa ona reorientacji na skrzydłach młodszych fałdów F<sub>2</sub>. Podczas etapu D<sub>2</sub> foliacja S<sub>1</sub> została zdeformowana w fałdy F<sub>2</sub> o osiach

NE-SW. Kliważ osiowy fałdów F<sub>2</sub> ma łagodne nachylenie ku W, SW lub NW. Miejscami ma formę kliważu krenulacyjnego, a miejscami tworzy nową penetratywną foliację S<sub>2</sub> zacierającą starsze powierzchnie S<sub>1</sub>. W efekcie przecięcia kliważu S<sub>2</sub> ze starszą foliacją S<sub>1</sub>, powstała penetratywna lineacja intersekccyjna L<sub>2</sub> o przebiegu NE-SW, będąca główną strukturą linijną w badanym terenie. Deformacja D<sub>3</sub> skoncentrowała się w strefach ścinania o upadzie ku SW, w których foliacja S<sub>3</sub> jest równoległa do S<sub>2</sub>, a lineacja z rozciągania L<sub>3</sub> jest równoległa do L<sub>2</sub>.

Analiza wskaźników kinematycznych dowodzi, że deformacja D<sub>1</sub> wiązała się z transportem tektonicznym ku E. Etap D<sub>2</sub> zachodził natomiast w efekcie koaksjalnego skrócenia o kierunku NW-SE. Konsekwencją rosnącego skrócenia było powstanie niskokątowych, normalnych stref ścinania D<sub>3</sub> o zwrocie "strop-ku-SW" lub "ku-WSW". W etapie D<sub>1</sub> jednostki tektoniczne Kamieńca i Chałupek nasunęły się kolejno na jednostkę Byczenia, co doprowadziło do tektonicznej inwersji stopnia metamorfizmu. W etapie D<sub>2</sub> powstała makrosyntforma F<sub>2</sub> o osi NE-SW. Jej krótsze skrzydło uległo silnemu skróceniu w kierunku pionowym. W etapie D<sub>3</sub> rozwinął się kolaps ekstensyjny ku SW, a wzdłuż wschodniej krawędzi bloku sowiogórskiego powstała przesuwca, lewoskrętna strefa dyslokacyjna Niemczy.

*Manuscript received 1 December 1997, accepted 17 February 1999*

## INTRODUCTION

The characteristics and history of tectonic deformation in rock complexes of the eastern part of the Fore-Sudetic Block have remained an object of mutually conflicting interpretations (Dziedzicowa, 1985, 1987; Cymerman & Jerzmański, 1987; Cymerman & Piasecki, 1994; Achramowicz, 1994; Mazur & Puziewicz, 1995a; Nowak, 1995). The controversy has concerned both the sequence and kinematics of ductile deformation events in that area. Our research on mica schists from the vicinity of Kamieniec Ząbkowicki (Fig. 1) was aimed at providing new constraints on the deformation history of the eastern part of the Fore-Sudetic area. Another objective was to integrate the data collected previously in the Niemcza Shear Zone and the Doboszowice Metamorphic Complex (Fig. 1). The new information obtained during our study allowed us to complete the earlier

interpretation of Mazur & Puziewicz (1995a) and to put forward a model explaining the tectonic evolution of the crystalline complexes located between the Góry Sowie Massif and Niedźwiedź Massif (Fig. 1).

## GEOLOGICAL SETTING AND PREVIOUS STUDIES

To the east of the Góry Sowie Massif and of the Niemcza Shear Zone there occurs a N-S elongated schist belt (Fig. 1). This schist belt is referred to, here, as the Kamieniec Ząbkowicki Metamorphic Complex. The northern part of the complex is aligned N-S that is along the eastern margin of the Niemcza Zone whereas its southern part forms an inlier in the vicinity of Kamieniec Ząbkowicki. The mica schists contain intercalations of quartzo-feldspatic schists

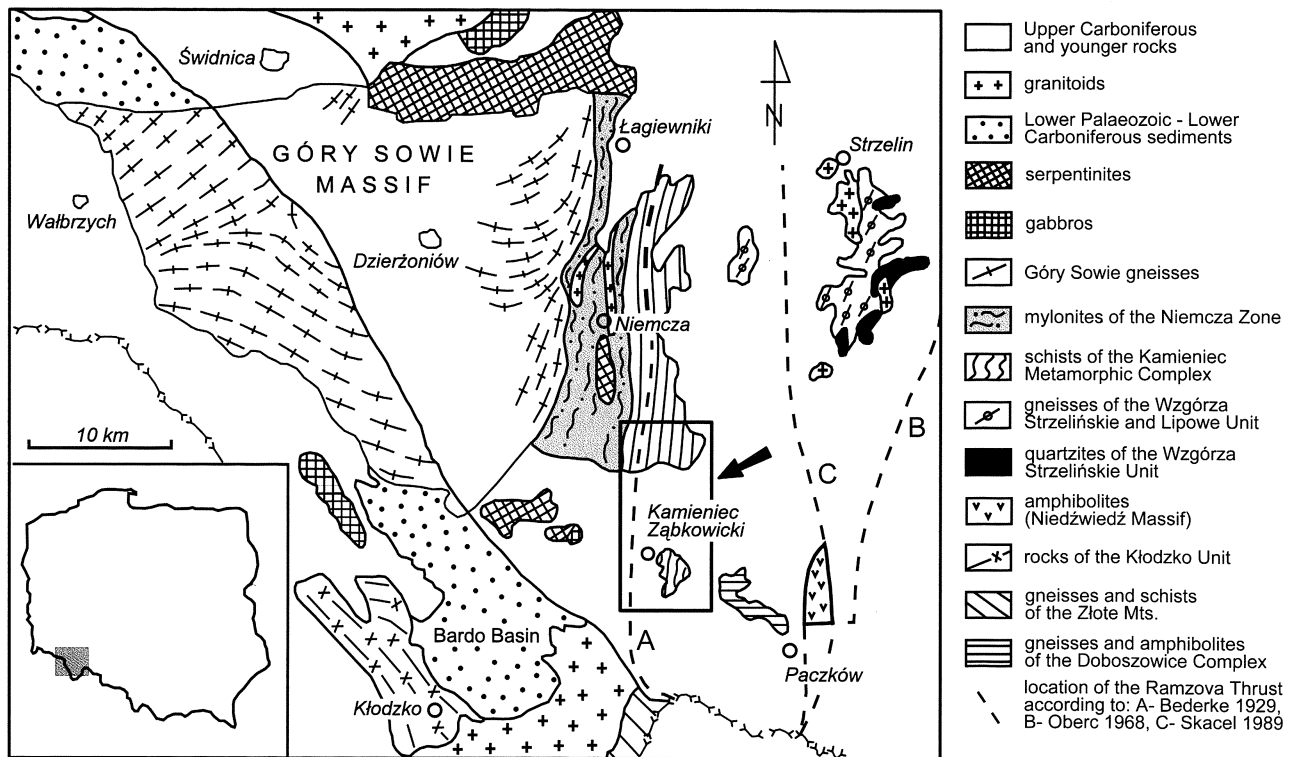
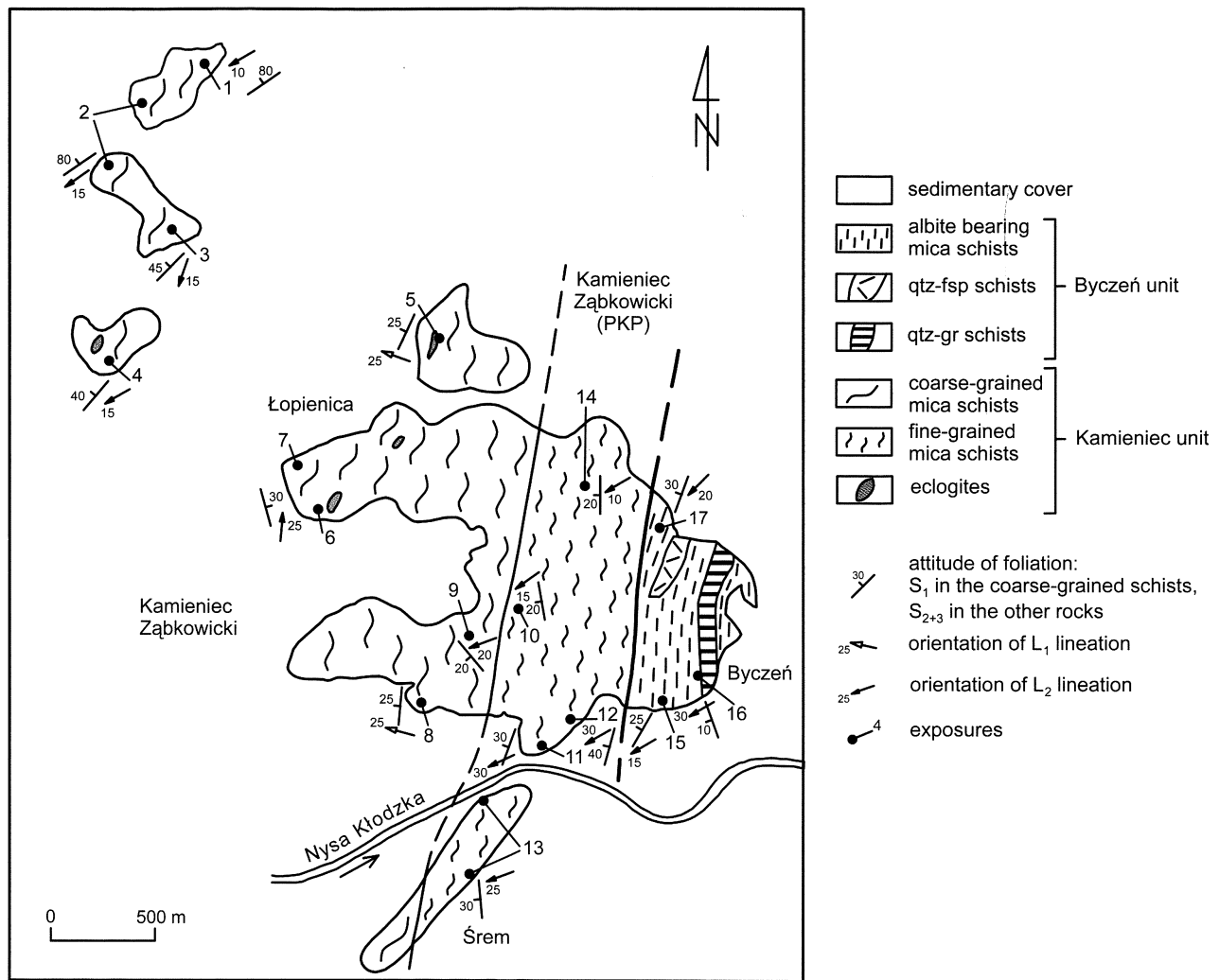


Fig. 1. Regional setting of the study area (box indicated by an arrow)



**Fig. 2.** Geological sketch map of the vicinity of Kamieniec Ząbkowicki modified after Baraniecki (1956) and Gaździk (1957) and location of the most important exposures

and marbles and subordinate lenses of quartzo-graphitic schists, amphibolitic schists and eclogites (Fig. 2, 3).

The penetrative foliation in the Kamieniec Ząbkowicki Metamorphic Complex dips to the SW, W and NW at variable angles. The dip of foliation increases westwards, towards the contact with the Niemcza Shear Zone (Mazur & Puziewicz, 1995b). The stretching lineation is, in general, plunging to the SW at a low angle.

The sequence of tectonic deformation in the Kamieniec Ząbkowicki Metamorphic Complex was previously studied by Dziedzicowa (1975, 1985, 1987) who distinguished three deformation events. The penetrative, almost vertical foliation  $S_1$  developed during the first event. This foliation was subsequently deformed by  $F_2$  folds which showed subhorizontal axial planes. Axial cleavage  $S_2$  of these folds locally obliterated the older foliation  $S_1$ . The last event,  $D_3$ , produced similar folds of almost vertical axial planes.

A different deformation sequence for mica schists from vicinities of Kamieniec Ząbkowicki was described recently by Achramowicz *et al.* (1997). In their interpretation, the first deformation event, related to SSW-directed thrusting, produced foliation  $S_1$ , which is now preserved exclusively

in eclogites. The succeeding events,  $D_2$  and  $D_3$ , are to represent the main deformations. The  $D_2$  event brought about normal dip-slip shear zones, characterised by a top-to-SW sense of ductile shear and was accompanied by high temperature metamorphism of upper amphibolite facies. The  $D_3$  deformation operated under dextral transpression regime. It was due to regional E–W shortening and resulted in easterly vergent thrusting followed by development of dextral strike-slip and/or wrench-normal faults. This deformation sequence (Achramowicz *et al.*, 1997) represented a modified version of earlier interpretations published by Achramowicz (1994) and Achramowicz *et al.* (1995).

A similar history of deformation is postulated by Nowak (1998). The earliest structures were defined, according to this author, by HP mineral assemblage and were probably related to the  $D_1$  thrusting. A subsequent exhumation was mostly related to low-angle normal faults ( $D_2$ ), and resulted in SW-vergent structures, coeval with emplacement of granitoid magmas (e.g. Strzelin–Żulova plutons). The temperature peak of metamorphism took place at the end of the  $D_2$  event. Further uplift and exhumation was associated with transpression and thrusting to the east ( $D_3$ ) in a colli-

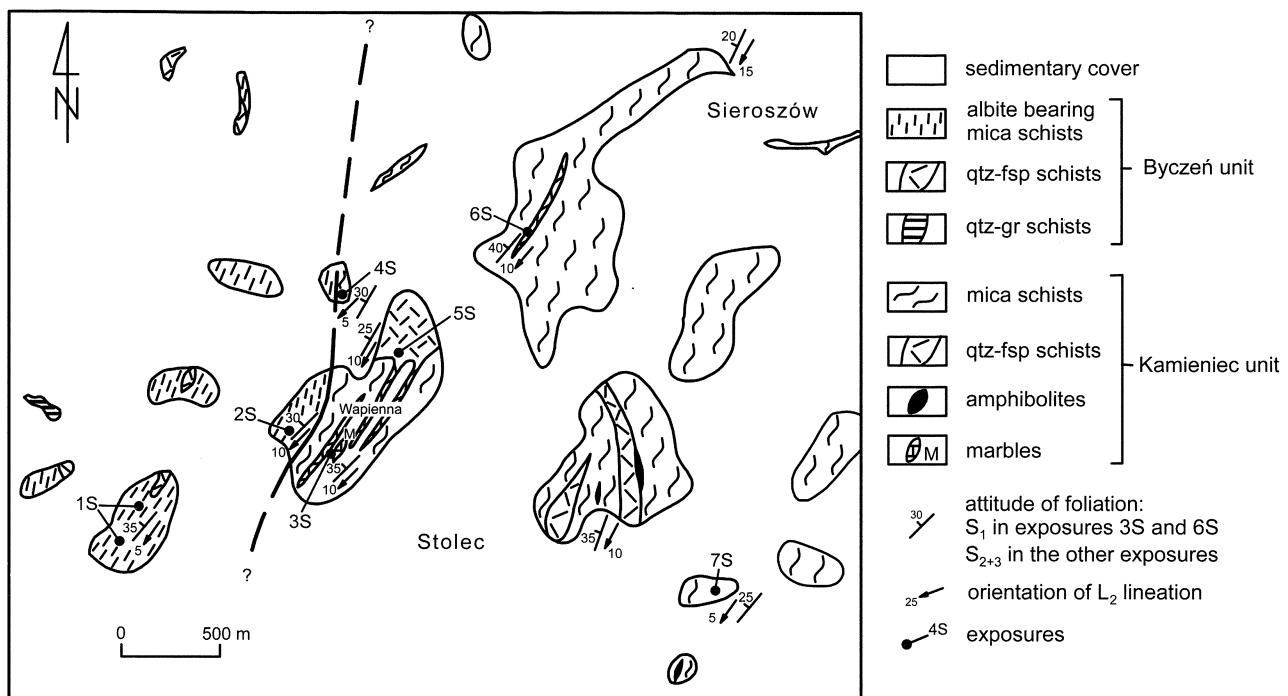


**Fig. 3.** Geological sketch map of the vicinity of Stolec modified after Badura (1979) and Badura & Dziemiańczuk (1981) and location of the most important exposures

sional setting between the Saxothuringian and Moravosilesian terranes. Late orogenic extension (D<sub>4</sub>) partly transposed the WSW-dipping S<sub>2</sub> foliation in shear zones under normal faulting regime.

A succession of four consecutive deformation events was suggested for the eastern part of the Fore-Sudetic block by Cymerman (1986, 1991) and Cymerman & Jerzmanowski (1987). In a more recent work, Cymerman and Piasecki (1994) suggest that deformation and metamorphism in that area were mainly related to the formation of NNE-directed overthrusts. This hypothesis reflects the recently widespread concept of tectonic evolution of the entire eastern margin of the Bohemian massif. This concept assumes that the nappe complexes of the Moldanubian zone and of the West Sudetes (Lugicum of Suess 1926) are overthrust towards the NE to NNE, on top of the Moravo-Silesian zone of the Variscides (Schulmann, 1991; Fritz & Neubauer, 1993; Schulmann *et al.*, 1995).

Recently, Mazur & Puziewicz (1995a) and Mazur *et al.* (1995) recognised three ductile deformation events, D<sub>1</sub>, D<sub>2</sub> and D<sub>3</sub>, in the metamorphic rocks east of the Góry Sowie Massif. The first two deformations D<sub>1</sub> and D<sub>2</sub> were related to nappe overthrusting towards the E and NE, respectively, under amphibolite facies conditions. They presumably represented the main contractional deformations on the eastern margin of the Bohemian Massif and were associated to regional thrusting of the West Sudetes over the East Sudetes. The D<sub>3</sub> event involved regional tectonic extension resulting in top-to-SW normal-slip shearing along slightly inclined foliation planes and sinistral strike-slip shearing along sub-vertical foliation planes (Mazur & Puziewicz, 1995a, b). The latter case corresponded to the regional-scale strike-slip Niemcza Shear Zone which developed along the eastern

margin of the Góry Sowie block during the D<sub>3</sub> event (Fig. 1). Penetrative mylonitization D<sub>3</sub> involved not only gneisses within the Niemcza Shear Zone but also mica schists in the adjacent part of the Kamieniec Complex (Mazur & Puziewicz 1995b). However, in the southern part of this complex Mazur & Puziewicz (1995a) and Mazur *et al.* (1995) observed only local D<sub>3</sub> shear zones cross-cutting the older pervasive D<sub>2</sub> fabric.

## METHODS

Our study is based on observations and measurements made in 42 exposures of mica schists from the vicinity of Kamieniec Ząbkowicki and in 10 exposures from the vicinities of Stolec. Locations of the most important exposures are shown on geological sketch maps (Figs 2, 3) and are compiled in Table 1. All microscopic observations and measurements were made using oriented thin sections cut parallel to the lineation and perpendicular to the foliation. 63 samples underwent microscopic examination: out of these 47 were collected in the vicinities of Kamieniec Ząbkowicki and 16 in the vicinity of Stolec. Kinematic analysis was focused on the evaluation of the sense of shear using meso- and microscopic indicators.

The orientation of quartz  $\langle c \rangle$  axis was measured on the universal stage in thin sections from 33 samples: 26 of them collected near Kamieniec Ząbkowicki and 7 coming from the vicinities of Stolec. In this paper we present 21 from among the total of 33 resultant stereograms. Preferred orientation of quartz  $\langle c \rangle$  axis was analysed since the mica schists of the study area show distinct differentiation among quartz and silicate layers and domains. In such a case quartz aggre-

**Table 1**

Location of exposures shown in the Figures 2 and 3

No of exp.	Location
1	Approximately 1.5 km north of Kamieniec Ząbkowicki, east of the railway to Jaworzyna Śląska, rocks at top of the hill 270.2 m
2	Approximately 1.5 km north of Kamieniec Ząbkowicki, to the west of the railway to Jaworzyna Śląska, steep scarp 50 m west of exposure 1
3	Small quarry approximately 800 m north of Kamieniec Ząbkowicki, SW slope of the hill 282.9 m
4	Quarry in the northern part of Kamieniec Ząbkowicki, near to railway viaduct
5	Small quarry near to the railway to Jaworzyna Śląska, 400 m west of Kamieniec Ząbkowicki railway station
6	Rocks at top of the hill 272.7 m in Kamieniec Ząbkowicki
7	Approximately 50 m north of exposure 6, quarry behind the houses in Łopienica
8	Approximately 1.5 km east of Kamieniec Ząbkowicki, scarp along the road towards Byczęń, near to the bridge across Budzówka brook
9	Small quarry on the north slope of Albert Hill, 20 m to the south of the tourist path from the castle to the temple, at top of the hill 290.6 m
10	Quarry on NW slope of the hill 300.2 m, approximately 30 m east of exposure 9 at the forest roads crossing
11	North scarp of the valley of the river Nysa Kłodzka in Byczęń
12	Quarry on the SW slope of the hill 308.0 m, at the periphery of Byczęń
13	Scarps and trenches on the west and east slopes of the hill 271.9 m, south bank of the river Nysa Kłodzka
14	Quarry at top of the hill 290.6 m, near to the temple
15	Quarry in Byczęń, 20 m west of the road to Kamieniec Ząbkowicki railway station
16	Quarry in Byczęń on SE slope of the hill 272.3 m
1S	West of Stolec, two small quarries on SW slope of the hill 353.0 m
2S	Small quarry to the west of Stolec, 100 m west of summit of Wapienna Hill (398.0 m)
3S	Large quarry on south slope of Wapienna Hill (398.0 m), west of Stolec
4S	Small crag between Wapienna Hill and the hill 341.8 m
5S	Quarry on NW slope of Wapienna Hill
6S	Quarry north of Stolec on west slope of the hill 377.6 m, near to the road to Sieroszów
7S	Quarry at top of the hill 357.5 m, east of Stolec

gates are appropriate for analysis of crystallographic orientation in spite of a high total content of micas in the rock (Walniuk & Morris, 1985). The orientation of  $\langle c \rangle$  axis was only measured in grains enclosed in monomineral quartz assemblages. In consequence, the influence of micas admixture on the deformation mechanism of quartz grains was minimised. In rock domains rich in mica flakes, quartz is deformed mainly by intercrystalline mechanisms: grain boun-

dary sliding and pressure solution due to high number of quartz-mica contacts (Starkey & Cutforth, 1978; Morris, 1978; Shelley, 1982). These mechanisms do not produce a lattice preferred orientation of quartz and the grains tend to remain strain-free (Nicholas & Poirier, 1976). On the other hand, monomineral quartz domains are deformed by intracrystalline mechanisms: dislocation glide and dislocation creep which result in a well-defined lattice orientation (Walniuk & Morris, 1985). Therefore, quartz  $\langle c \rangle$  axis patterns obtained for monomineral quartz domains are useful for analysis of deformation kinematics in the study mica schists.

## LITHOLOGY AND PETROGRAPHY

### VICINITIES OF KAMIELEC ZĄBKOWICKI

Mica schists from the vicinities of Kamieniec Ząbkowicki (Fig. 2: exposures 1–14) are composed of quartz, muscovite, biotite, garnet, plagioclase (10–25% An), andalusite, staurolite and chlorite. Accessory minerals are tourmaline, apatite, zircon, allanite, rutile, and ilmenite. The mica schists comprise two main structural varieties: coarse- and fine-grained schists (Józefiak, 1995).

The fine-grained schists (exp. 10–14) are differentiated into regularly alternating quartz-muscovite and muscovite-biotite laminae whereas the coarse-grained schists (exp. 1–9) consist of elongated quartz aggregates enveloped by muscovite-biotite layers. Irregular muscovite concentrations, up to 25 mm long, are locally present in both varieties of mica schists. Individual muscovite grains within these aggregates are isometric or slightly elongated and display random orientation.

Mica layers in both varieties of schists contain numerous garnet porphyroblasts up to 3 mm across in the fine-grained and up to 4–10 mm across in the coarse-grained variety. Staurolite, chlorite, plagioclase and andalusite represent significant, but less frequent components of the mica layers. Most garnet crystals in the coarse-grained schists are replaced by pseudomorphs of biotite, chlorite, muscovite, plagioclase, staurolite and of iron hydro-oxides which include small relics of garnet. Linear and S-shaped inclusion trails are still visible in less altered garnets from coarse- and fine-grained mica schists. Inclusion trails contain mainly rutile, ilmenite, quartz and subordinate chloritoide, staurolite, chlorite, kyanite, margarite, paragonite, muscovite and tourmaline. Well-developed pressure-shadows around garnets are filled with quartz, muscovite, biotite and, infrequently, with plagioclase and staurolite.

The mica schists from the vicinities of Kamieniec Ząbkowicki contain all three polymorphs of  $\text{Al}_2\text{SiO}_5$ . The coarse-grained schists comprise post-kinematic crystals of andalusite up to 6 mm long. They enclose numerous muscovite, biotite, quartz, staurolite, plagioclase, ilmenite and rutile inclusions aligned parallel to the foliation planes. In places, andalusite overgrows margins of partly altered garnet porphyroblasts. Syn- to post-kinematic andalusite grains (up to 1 mm) occur, in the fine-grained schists, as well. They are often deformed and, less frequently, contain spiral inclusion trails. Scarce sillimanite is represented by intergrowths

of fibrolite in muscovite, garnet and quartz. Fibrolite is also visible in pressure shadows of staurolite grains and around analusite porphyroblasts. Prismatic crystals of sillimanite are only locally present in the coarse-grained schists, enclosed within muscovite aggregates. Kyanite was found only as intergrowths in garnet in the coarse-grained mica schists. Dziedzicowa (1966) and Nowak (1995) described scarce individual grains of this mineral occurring within mica layers.

Plagioclase (10–25% An) in the coarse-grained schists forms large crystals up to 4 mm long, lengthened parallel to the foliation. Smaller grains make up elongated aggregates together with mica plates, iron oxides and, locally, with andalusite crystals. In the fine-grained schists small plagioclase grains (10–25% An) occur within mica layers. Locally, in both varieties of mica schists oligoclase is accompanied by albite blasts.

Staurolite is present only in some parts of mica shists within mica layers or muscovite aggregates. Its prismatic crystals are 0.1 mm to 0.7 mm long. Numerous randomly oriented staurolite grains together with these of muscovite and biotite define, in places, thin elongated trails, which envelope garnet porphyroblasts.

Chlorite represents only a subordinate component of mica layers. Its grains usually parallel foliation but, locally, display random orientation. Chlorite is the dominant mineral phase in most pseudomorphs substituting garnet porphyroblasts.

### Vicinities of Byczęń

Fine-grained mica schists containing albite crop out in the vicinities of Byczęń (Fig. 2). In contrast to mica schists from the vicinities of Kamieniec Ząbkowicki, they contain numerous porphyroblasts of albite (Fig. 4) and are devoid of staurolite and andalusite. Albite-bearing mica schists are composed of alternating quartz and mica layers and of fine-grained matrix. The latter consists of numerous mica and chlorite flakes scattered among smaller grains of quartz and plagioclase (20–24% An). Accessory minerals are tourmaline, apatite and opaques. Both in the fine-grained matrix

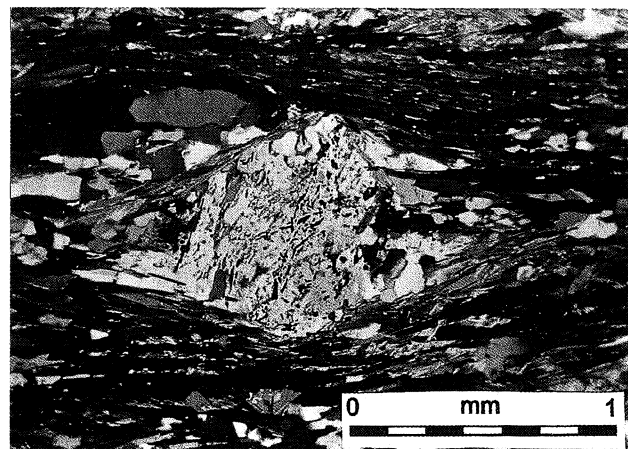


**Fig. 4.** Synkinematic albite porphyroblast in mica schist (Byczęń unit)

and in mica layers, there occur few relics of garnet. They are preserved as irregular clasts or as small remains within pseudomorphs. Very small garnet blasts, below 0.05 mm across, are locally visible.

### Vicinities of Stolec

Mica schists from the vicinities of Stolec (Fig. 3) are characterised by a significant variation of structure and mineral composition. The fine-grained mica schists of monotonous composition crop out to the west of Stolec (exp. 1S and 2S). They consist mainly of quartz, muscovite, biotite and plagioclase (15–30% An). Accessory minerals are represented by tourmaline, apatite (locally up to 3.5 mm long) and opaques. Their planar fabric is defined by mica layers and quartz lenses alternating with the fine-grained matrix composed of quartz, plagioclase and mica. Some horizons of mica schists contain numerous porphyroblasts of synkinematic albite, up to 3 mm in diameter.

To the west and north of Stolec (exp. 6S, 7S) the mica schists display medium-grained structure and more diversified composition. In addition to quartz, muscovite, biotite and plagioclase, these rocks are rich in garnet, staurolite and chlorite. Andalusite and sillimanite represent their less abundant components. Staurolite prisms, up to 1 mm long, occur in the mica layers. They locally cluster in elongated concentrations parallel to foliation planes. Garnet forms porphyroblasts reaching up to 4 mm across. They contain numerous S-shaped or spiral inclusion trails. Inclusions contain mainly quartz and opaques but less frequent rutile and plagioclase are also present. Few andalusite prisms are up to 1 mm long. They display random orientation with respect to foliation.

Locally, north of Wapienna hill (exp. 4S), mica schists contain synkinematic chlorite, which is accompanied by green biotite, andalusite, staurolite and garnet. Plagioclase (1–14% An) represents only subordinate mineral phase. Andalusite blasts in this variety of mica schists display clearly synkinematic character. They enclose S-shaped or spiral trails of quartz and ilmenite inclusions.

## METAMORPHISM

According to Dziedzicowa (1966), the Kamieniec Ząbkowicki Metamorphic Complex consists of two contrasting domains: the north-western and the eastern one. The former is composed of mica schists locally containing garnet and sillimanite, whereas the latter comprises mica schists of more varied mineral composition, including garnet, staurolite, andalusite and kyanite. Crystallization of andalusite probably post-dated the origin of kyanite (Dziedzicowa 1987). The temperature and pressure of metamorphism in the mica schists near to Kamieniec Ząbkowicki is estimated by Dziedzicowa (1973) at 550–570°C and 6.5 kbar.

Nowak (1995, 1998) suggested that consecutive tectonic deformations were accompanied in the mica schists by a clockwise P-T path with a pressure peak in its earlier stage and a temperature peak during the later events. This path indicates compression and crustal thickening during the initial

stage of metamorphism, continuing until pressure peak conditions were achieved during the continental collision. The minimum pressure and temperature conditions for the peak of pressure were estimated by Nowak at 11–12 kbar and 400–430°C. A subsequent decompression took place under conditions of rising temperature, in the amphibolite facies field, ultimately reaching the temperature peak under the conditions of 579 ±35°C and 7.4 ±0.2 kbar. After the temperature peak of metamorphism was achieved, further decompression was almost isothermal up to the andalusite stability field. A record of early HP metamorphism, inferred for mica schists, is preserved in eclogites from the vicinities of Kamieniec Ząbkowicki which were metamorphosed under temperature of ±575°C and pressure of 15 kbar (Achramowicz, 1997).

Recent investigations of Józefiak (1994, 1996) indicate that coarse- and fine-grained mica schists preserved record of different metamorphic conditions. The coarse-grained schists achieved peak metamorphism conditions under a temperature of 570–640°C and pressure of 8–13 kbar (mineral assemblage Ms+Bt+Grt+Pl±St±Ky±Cld), whereas the fine-grained schists recorded a temperature of 510–540°C and pressure of 7.0–8.5 kbar. Mica schists in close proximity to eclogites preserved evidence for a higher grade metamorphism under a temperature of 610–630°C and pressure of 10–13 kbar. The final metamorphic event in both varieties of mica schists is represented by the mineral assemblage Ms+Bt+Grt+Pl+And±Sil±St. The temperature and pressure during this event were characterised by the occurrence of andalusite which was locally replaced by sillimanite. The stability field of this assemblage corresponds to a temperature above 530°C and pressure below 4 kbar.

## DEFORMATION

Three generations of deformational structures were recognised in the mica schists from the vicinities of Kamieniec Ząbkowicki. They are interpreted as reflecting three deformation events D<sub>1</sub>, D<sub>2</sub> and D<sub>3</sub> of regional extent. Numbering of the distinguished deformation stages refers to the scheme adopted in the earlier papers of Mazur & Puziewicz (1995) and Mazur *et al.* (1995). The first, D<sub>1</sub>, deformation produced foliation S<sub>1</sub> and lineation L<sub>1</sub>. The next, D<sub>2</sub>, event resulted in development of F<sub>2</sub> folds, crenulation cleavage and foliation S<sub>2</sub> and lineation L<sub>2</sub>. The latest deformation, D<sub>3</sub>, gave rise to the origin of lineation L<sub>3</sub> and foliation S<sub>3</sub>, in general parallel to S<sub>2</sub>.

Structural observations from the neighbourhood of Kamieniec Ząbkowicki show that foliation S<sub>1</sub> and lineation L<sub>1</sub> are penetrative in the coarse-grained mica schists whereas the younger foliation S<sub>2+3</sub> is dominant in the fine-grained schists. Our division of mica schists into the coarse- and fine-grained varieties (Fig. 2) is, therefore, consistent with structural data concerning a type of development of the penetrative foliation.

The coarse-grained mica schists are exposed in the vicinities of Kamieniec Ząbkowicki whereas the fine-grained schists crop out around Byczęń (Fig. 2). Locally, bands of fine-grained schists, up to few tens of metres thick, occur

within the coarse-grained variety (exposure 4). Further to the north, in the vicinities of Stolec (Fig. 3), no interrelationship between the size of grain and the type of a penetrative foliation can be observed. An equivalent of the coarse-grained rock variety in that area is represented by mica schists exposed on the Wapienna Hill (exp. 3S, 6S). The latter rocks are characterised by penetrative foliation S<sub>1</sub>. On the contrary, in other mica schists cropping out around Stolec (Fig. 3), foliation S<sub>2+3</sub> is the dominant planar structure, similarly as in the fine-grained schists. Consequently, the characteristics of the coarse- and fine-grained varieties of mica schists presented below are extended to include their structural equivalents in the vicinities of Stolec.

### Deformation D<sub>1</sub>

The foliation of the coarse-grained mica schists (S<sub>1</sub>) is defined by alternation of quartz and mica layers and by parallel alignment of mica plates. Foliation S<sub>1</sub> displays a variable attitude (Fig. 2) since it mostly dips to the NW at high to moderate angles (exp. 1, 2, 3) or shows gentle eastward inclination (exp. 6, 7). The orientation of foliation S<sub>1</sub> shown on stereograms (Fig. 5a, b) displays a great-circle girdle distribution around an axis plunging gently to the WSW (exp. 1, 2) or to NE (exp. 6, 7). This orientation distribution results from reorientation of S<sub>1</sub> on limbs of F<sub>2</sub> folds. A constant orientation of S<sub>1</sub> can be observed only in exposures 5, 8 and 9 which are located near the contact with fine-grained schists (Fig. 2). In these three localities, foliation S<sub>1</sub> dips gently towards the W (Fig. 6a, b). Stretching lineation L<sub>1</sub> is defined by elongation of mica aggregates and quartz rods on foliation S<sub>1</sub>. The general trend of the L<sub>1</sub> lineation is W–E to WNW–ESE (Fig. 7b). Most often the lineation L<sub>1</sub> is entirely obliterated by a younger lineation, L<sub>2</sub>, which represents the dominant linear structure in the coarse-grained schists. Lineation L<sub>1</sub> is reoriented on limbs of the F<sub>2</sub> folds. Therefore, its orientation shown on stereograms (Fig. 5c, 7b) is scattered along circles around the axis parallel to the axis of the foliation girdle. On steeper limbs of the F<sub>2</sub> folds (dipping to the NW) lineation L<sub>1</sub> plunges towards the west at moderate angles, whereas on less inclined limbs (dipping to the SE) L<sub>1</sub> trends WNW–ESE (Fig. 5c). The maximum on stereoplots which represents the lineation of gentle plunge towards the WNW, is dominant on the synoptic diagram of L<sub>1</sub> structures since the majority of measurements were collected in exposures 5 and 8 characterised by a shallow dip of foliation S<sub>1</sub> (Fig. 6). For the same reason the main maximum on the synoptic diagram of S<sub>1</sub> planes represents foliation dipping to the W at a low angle (Fig. 7a). In the vicinities of Stolec (exp. 3S and 6S), foliation S<sub>1</sub> is scattered along a girdle around the axis trending NE–SW (Fig. 8a). The dominant orientation of S<sub>1</sub> in that area is represented by foliation dipping steeply to the NW.

Numerous large garnet porphyroblasts occur in the coarse-grained mica schists. They display features suggesting synkinematic growth during the deformation D<sub>1</sub>. Their growth is indicated by sigmoidal inclusion trails (Fig. 9b) visible in many porphyroblasts. A synkinematic origin of garnet crystals is also evidenced, following Bell *et al.* (1986), by the presence of straight-line inclusion trails which

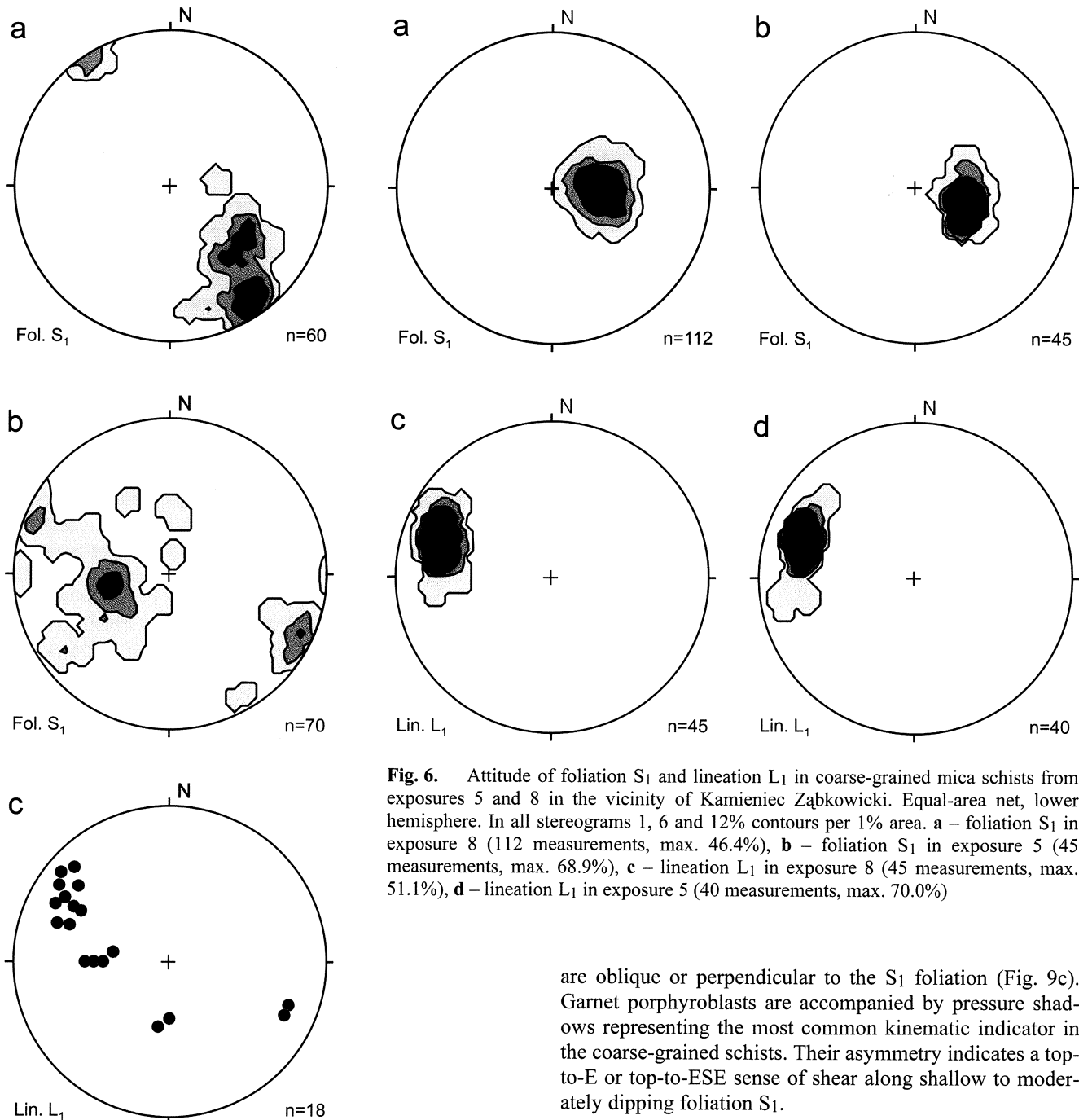


**Fig. 5.** Attitude of foliation  $S_1$  and lineation  $L_1$  in coarse-grained mica schists from exposures 1, 2, 6 and 7 in the vicinity of Kamieniec Ząbkowicki. Equal-area net, lower hemisphere. In stereograms **a** and **b** 1, 6 and 12% contours per 1% area. **a** – foliation  $S_1$  in exposures 1 and 2 (60 measurements, max. 26.7%), **b** – foliation  $S_1$  in exposures 6 and 7 (70 measurements, max. 17.1%), **c** – lineation  $L_1$  in exposures 1, 2, 6 and 7 (18 measurements)

**Fig. 6.** Attitude of foliation  $S_1$  and lineation  $L_1$  in coarse-grained mica schists from exposures 5 and 8 in the vicinity of Kamieniec Ząbkowicki. Equal-area net, lower hemisphere. In all stereograms 1, 6 and 12% contours per 1% area. **a** – foliation  $S_1$  in exposure 8 (112 measurements, max. 46.4%), **b** – foliation  $S_1$  in exposure 5 (45 measurements, max. 68.9%), **c** – lineation  $L_1$  in exposure 8 (45 measurements, max. 51.1%), **d** – lineation  $L_1$  in exposure 5 (40 measurements, max. 70.0%)

are oblique or perpendicular to the  $S_1$  foliation (Fig. 9c). Garnet porphyroblasts are accompanied by pressure shadows representing the most common kinematic indicator in the coarse-grained schists. Their asymmetry indicates a top-to-E or top-to-ESE sense of shear along shallow to moderately dipping foliation  $S_1$ .

#### Deformation D<sub>2</sub>

Foliation  $S_1$  is deformed by mesoscopic F<sub>2</sub> folds of amplitude ranging from several dozen of centimetres to few metres. F<sub>2</sub> axes trend NE–SW, parallel to lineation  $L_2$ , with their axial planes dipping gently to the NW or SE. In the exposures located around Stolec and to the west of Kamieniec Ząbkowicki (e.g. exp. 6, 3S), the F<sub>2</sub> folds are recumbent and display distinct NW asymmetry. Their longer limbs dip to the NW, whereas the shorter limbs are slightly inclined to the SE (Fig. 10). In exposures located near to the boundary between the coarse- and fine-grained mica schists (e.g. exp. 8), the F<sub>2</sub> folds are tight or almost isoclinal and their asymmetry is less apparent. The axial cleavage of the F<sub>2</sub> folds is represented by crenulation cleavage  $S_2$ . In the longer limbs

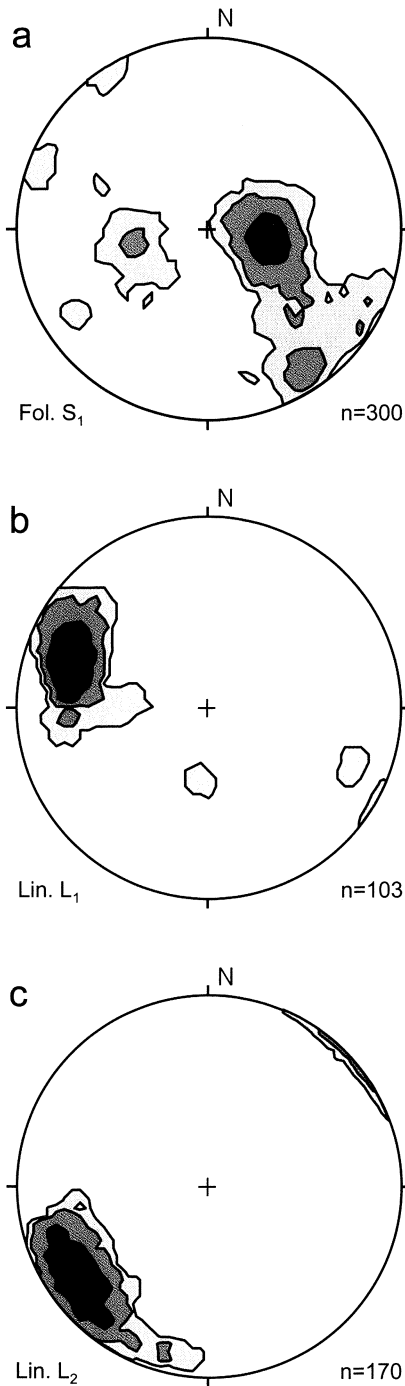


**Fig. 7.** Synoptic stereograms of foliation S<sub>1</sub>, lineation L<sub>1</sub> and lineation L<sub>2</sub> in coarse-grained mica schists from the vicinity of Kamieniec Ząbkowicki. Equal-area net, lower hemisphere. In all stereograms 1, 3 and 12% contours per 1% area. a – foliation S<sub>1</sub> (300 measurements, max. 26.3%), b – lineation L<sub>1</sub> (103 measurements, max. 48.5%), c – lineation L<sub>2</sub> (170 measurements, max. 32.9%)

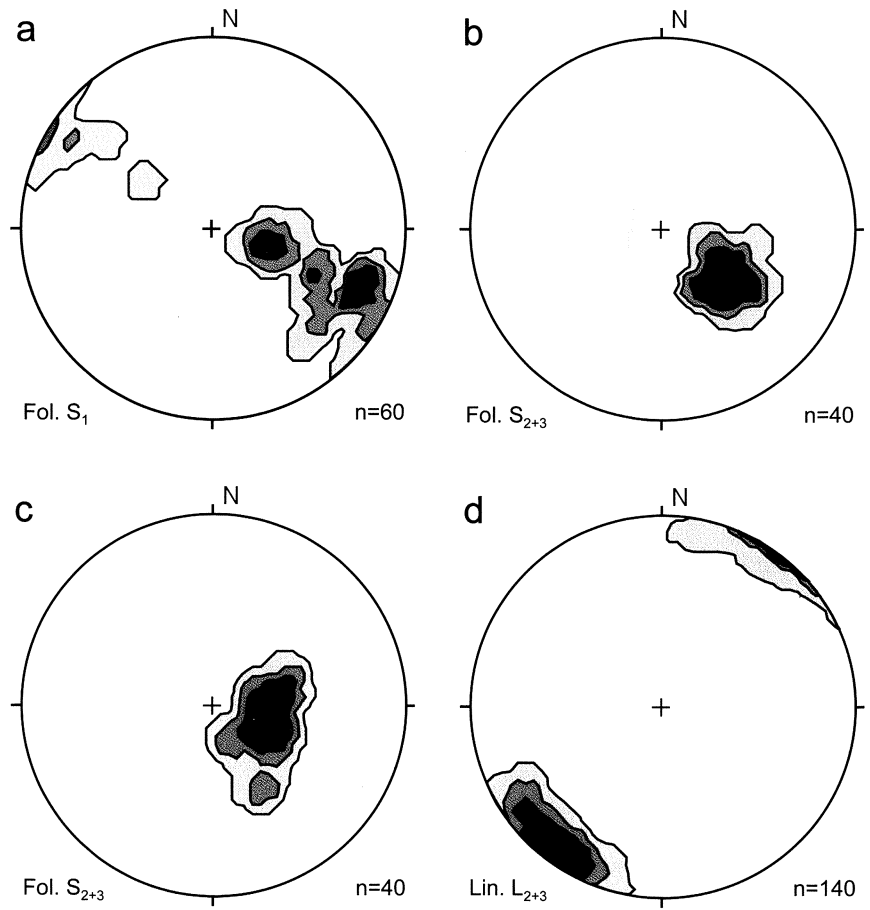


**Fig. 8.** Attitude of foliation and lineation in mica schists from the vicinity of Stolec. Equal-area net, lower hemisphere. In all stereograms 1, 6 and 12% contours per 1% area. a – foliation S<sub>1</sub> in the mica schists from exposures 3S and 6S (60 measurements, max. 23.3%), b – foliation S<sub>2+3</sub> in the mica schists from exposures 1S and 2S (40 measurements, max. 50%), c – foliation S<sub>2+3</sub> in the mica schists from exposure 7S (40 measurements, max. 40%), d – lineation L<sub>2+3</sub> from all exposures (140 measurements, max. 49.2%)

of folds (inclined to NW) the cleavage S<sub>2</sub> dips approximately to the S at a low angle whereas in the shorter limbs (inclined to E or SE) it is dipping towards the N (Fig. 10, 11). Variable dip of the cleavage in the hinges and limbs of asymmetric F<sub>2</sub> folds results from its fan-like orientation. On the contrary, in the hinges of tight or isoclinal F<sub>2</sub> folds, cleavage S<sub>2</sub> displays approximately constant orientation dipping gently to the W or NW, parallel to the axial planes of folds.

Variable orientation of the foliation S<sub>1</sub> (Fig. 5, 7, 8) shows that the F<sub>2</sub> folds reach the size exceeding a scale of individual exposures. Their axes plunge gently to the SW (WSW) or to the NE, comparable to the axes of girdles on foliation stereograms (Fig. 5, 8). The distribution of maxima on foliation S<sub>1</sub> stereograms (Fig. 5, 8) indicates the NW asymmetry of the map-scale F<sub>2</sub> folds, similar to the asymmetry of mesoscopic folds (Fig. 10). The poles to the foliation are clustered in two maxima lying on a great-circle girdle. The two maxima represent planes dipping steeply to the NW and gently to the SE or NW which correspond to the longer and shorter limb of folds, respectively. The NW asymmetry of the F<sub>2</sub> folds is also indicated by geometric re-

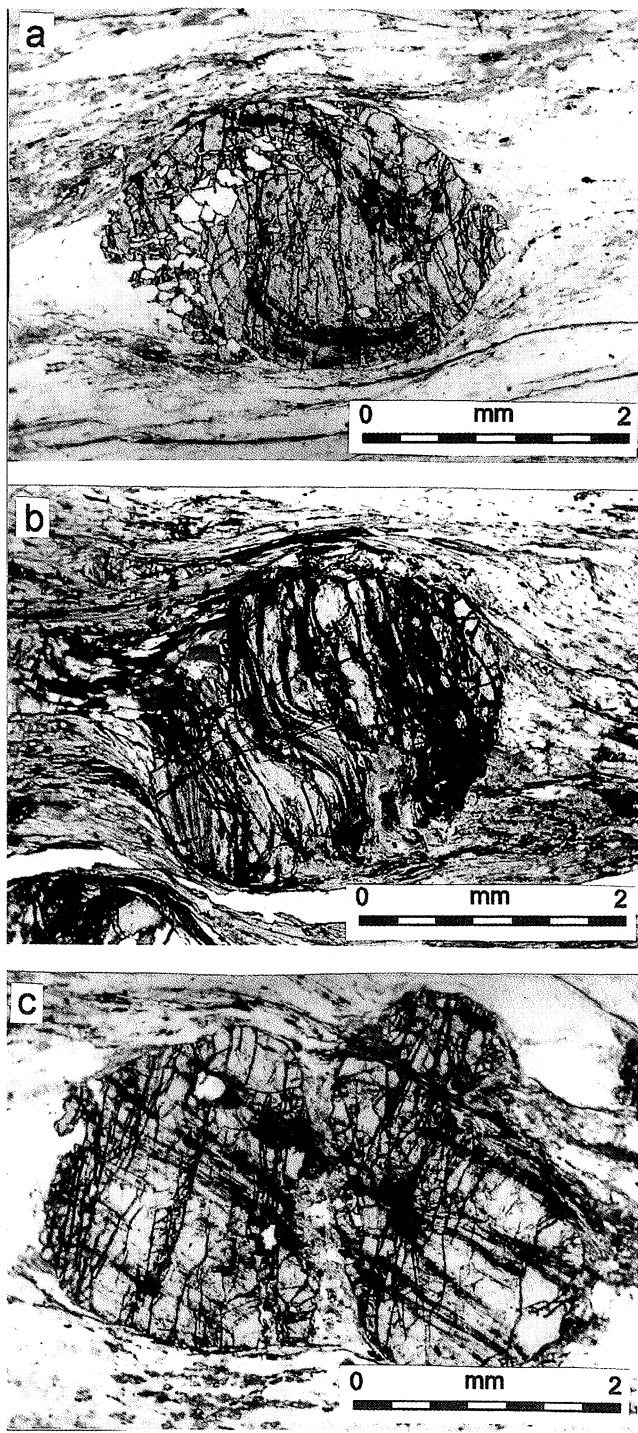


**Fig. 9.** Shape varieties of inclusion trails in garnet porphyroblasts: **a** – spiral inclusion trails, **b** – sigmoidal inclusion trails, **c** – straight-line inclusion trails

lationship between the foliation  $S_1$  and cleavage  $S_2$ . Most localities expose longer NW limbs of the folds (foliation  $S_1$  steeper than cleavage  $S_2$ ) whereas exposures showing shorter SE limbs (cleavage  $S_2$  steeper than foliation  $S_1$ ) are less frequent. The two maxima on a stereogram in Figure 11 represent different orientation of cleavage  $S_2$  on the opposite limbs of  $F_2$  folds.

Consecutive stages of development of planes  $S_2$  from crenulation cleavage to new foliation were found in the rocks (Fig. 12). In the coarse-grained variety of schists, the

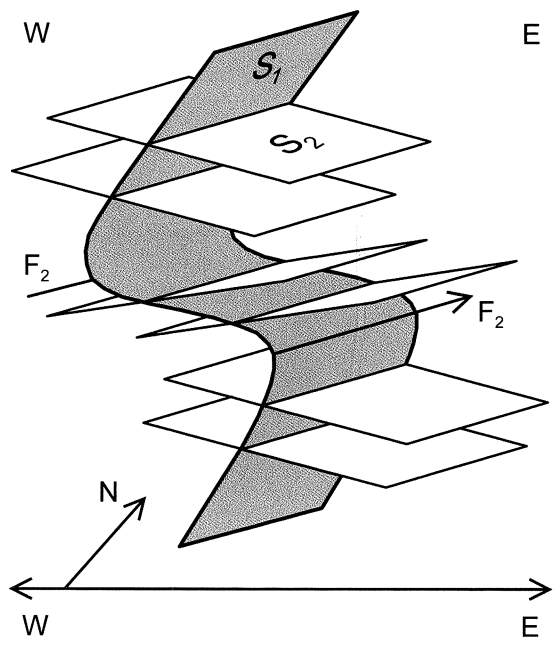


**Fig. 10.** Geometry of  $F_2$  folds of NW asymmetry and axes trending NE–SW to ENE–WSW. Cleavage  $S_2$  is slightly inclined to SW in steep limbs of folds and to NNW in the shorter, subhorizontal limbs

foliation  $S_1$  is deformed by tight symmetric folds with sharp hinges and the amplitude ranging from 1 to 20 mm. Axial planes of these folds correspond to the  $S_2$  crenulation cleavage. The  $S_2$  planes are locally imprinted by parallel alignment of micas (Fig. 12a) but, generally, they do not obliterate the older,  $S_1$ , foliation. In contrast, the  $S_2$  planes represent the main penetrative foliation in the fine-grained mica schists. New foliation  $S_2$  is defined in these rocks by alternation of mica and quartz-mica layers and by parallel alignment of individual micas. Mica layers correspond to the cleavage domains whereas relics of the older foliation  $S_1$  are still preserved in quartz-mica laminae (Fig. 12b). In the most strained portions of the fine-grained mica schists the foliation  $S_1$  is preserved only as inclusion trails in porphyroblasts and as isolated hinges of intrafolial folds (Fig. 13). The latter folds represent micro- or mesoscopic isoclinal structures developed due to the deformation of individual quartz laminae. Their axial planes parallel the foliation  $S_2$ .

The penetrative foliation  $S_2$  remains constantly oriented throughout the whole area. It dips consequently to the WNW at a low angle (Fig. 8, 14). It is thus parallel to orientation of  $F_2$  axial planes. On the stereograms (Fig. 11), the transposition foliation  $S_2$  shows no scatter characteristic for the crenulation cleavage in the coarse-grained mica schists.

The lineation  $L_2$  includes stretching lineation defined by alignment of micas and intersection lineation formed in the coarse-grained mica schists by intersection of the foliation  $S_1$  and the cleavage  $S_2$ . The orientation of  $L_2$  in the study area is fairly constant (Fig. 7c, 8, 14). The lineation  $L_2$  trends NE–SW or ENE–WSW, approximately parallel to hinges of  $F_2$ , and plunge gently to the SW or WSW. There is no difference between the orientation of  $L_2$  in the coarse- and fine-grained mica schists. On the  $S_1$  foliation planes,

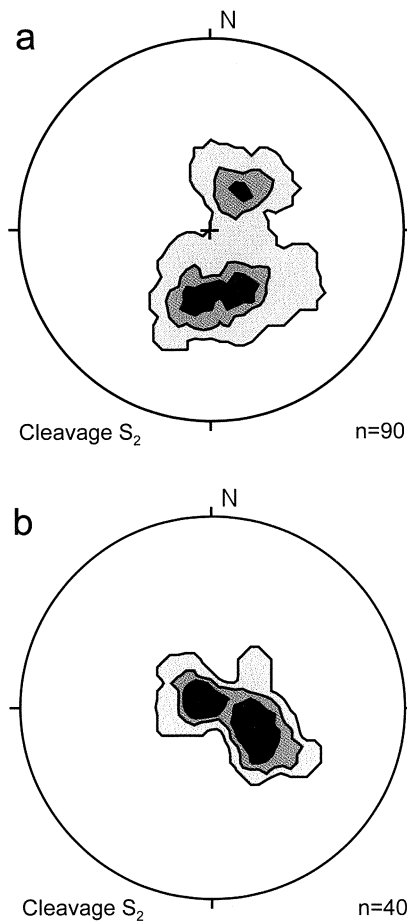


**Fig. 11.** Attitude of crenulation cleavage  $S_2$  in coarse-grained mica schists. Equal-area net, lower hemisphere. In all stereograms 1, 6 and 12% contours per 1% area. **a** – crenulation cleavage  $S_2$  in the vicinity of Kamieniec Ząbkowicki (90 measurements, max. 17.8%), **b** – crenulation cleavage  $S_2$  in the vicinity of Stolec – exposures 3S and 6S (40 measurements, max. 35%)

lineation  $L_2$  almost entirely obliterates the older lineation  $L_1$ . A superposition of both lineations,  $L_1$  and  $L_2$ , is visible only locally. The trend of  $L_1$  is usually closer to the E–W direction than that of  $L_2$  lineation.

Numerous garnet porphyroblasts occur in the fine-grained mica schist. Most of them are synkinematic with respect to the  $D_2$  deformation (Fig. 9). The most spectacular evidence for synkinematic development of garnet is provided by porphyroblasts with overgrown crenulations of the  $S_1$  foliation still preserved inside them as inclusion trails (Fig. 15a). In many other porphyroblasts the inclusion trails are spiral (Fig. 9a) or sigmoidal which can also be considered as an evidence for synkinematic growth (Bell *et al.*, 1986) concurrent with the development of the  $S_2$  foliation. On the other hand, structural observations cannot exclude that some garnet crystals represent porphyroclasts grown during the earlier  $D_1$  deformation. First of all, it applies to highly flattened grains of this mineral. Less common plagioclase and staurolite porphyroblasts also developed during the  $D_2$  event. Some of them contain inclusion trails of sigmoidal shape or representing crenulations of older foliation  $S_1$ . The garnet porphyroblasts are accompanied by pressure

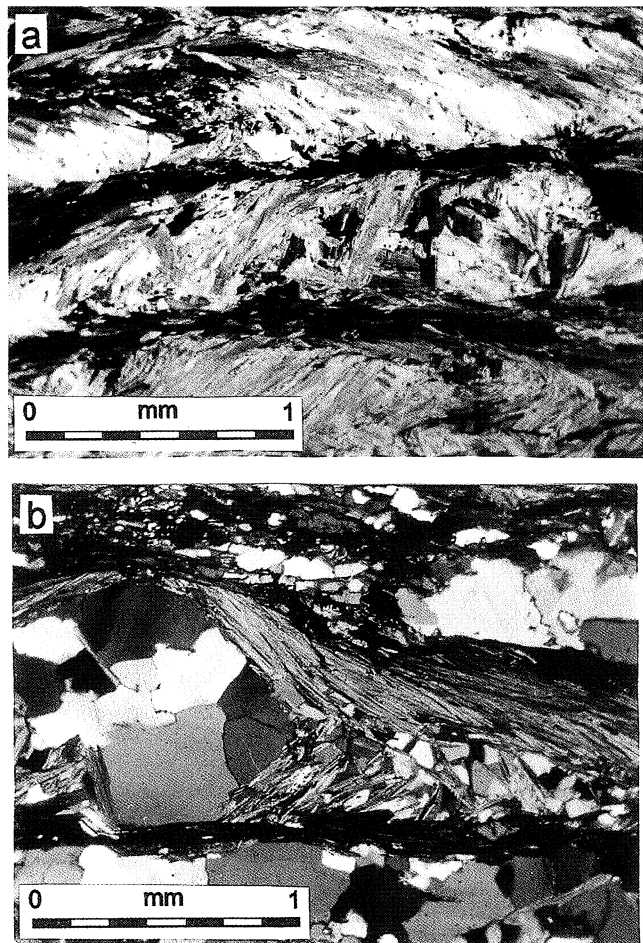


**Fig. 12.** Foliation  $S_1$  preserved in microlithons between younger foliation planes  $S_2$ : **a** – foliation  $S_2$  (horizontal on the photo) developed parallel to axial planes of crenulations of foliation  $S_1$  in coarse-grained schist, **b** – foliation  $S_1$  in fine-grained schist preserved in the hinge of a crenulation micro-fold in foliation  $S_2$  (horizontal on the photo)

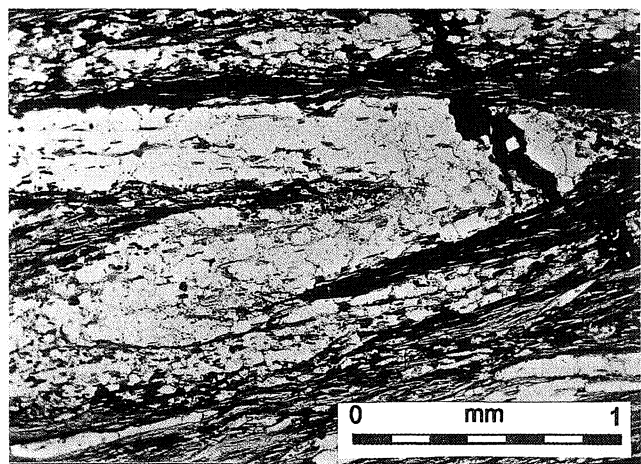


**Fig. 13.** Intrafolial fold in fine-grained schist. Folded foliation  $S_1$  is preserved between planes of penetrative foliation  $S_2$

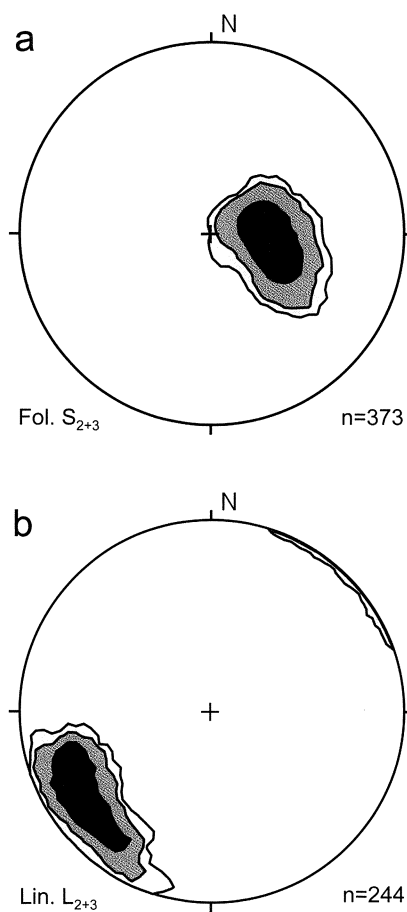


**Fig. 14.** Attitude of foliation S<sub>2+3</sub> and lineation L<sub>2+3</sub> in fine-grained mica schists from vicinities of Kamieniec Ząbkowicki and Byczęń. Equal-area net, lower hemisphere. In both stereograms 1, 3 and 12% contours per 1% area. **a** – foliation S<sub>2+3</sub> (373 measurements, max. 33.5%), **b** – lineation L<sub>2+3</sub> (244 measurements, max. 34.0%)

shadows which represent the most common kinematic indicator in fine-grained mica schists. Approximately symmetric pressure shadows indicate that some portions of fine-grained mica schists were subjected to mostly coaxial deformation during the D<sub>2</sub> event. In the mica schists showing approximately symmetric fabric, relics of older foliation S<sub>1</sub> are still preserved as hinges of crenulations between planes of the S<sub>2</sub> foliation (Fig. 12b). They suggest that crenulation cleavage was transformed into the foliation S<sub>2</sub> due to coaxial shortening.

The albite-bearing fine-grained mica schists exposed in the vicinity of Byczęń and to the west of Stolec do not differ structurally from other fine-grained schists. Essentially different is, however, the synkinematic mineral assemblage related to the D<sub>2</sub> deformation event in these rocks. The most important component of this assemblage is represented by numerous albite porphyroblasts (Fig. 4). They often contain sigmoidal inclusion trails suggesting synkinematic growth, contemporaneous with the development of penetrative S<sub>2</sub> foliation. On the other hand, few garnet grains, up to 2 mm across, display features of porphyroclasts and they probably crystallised during the previous D<sub>1</sub> event.

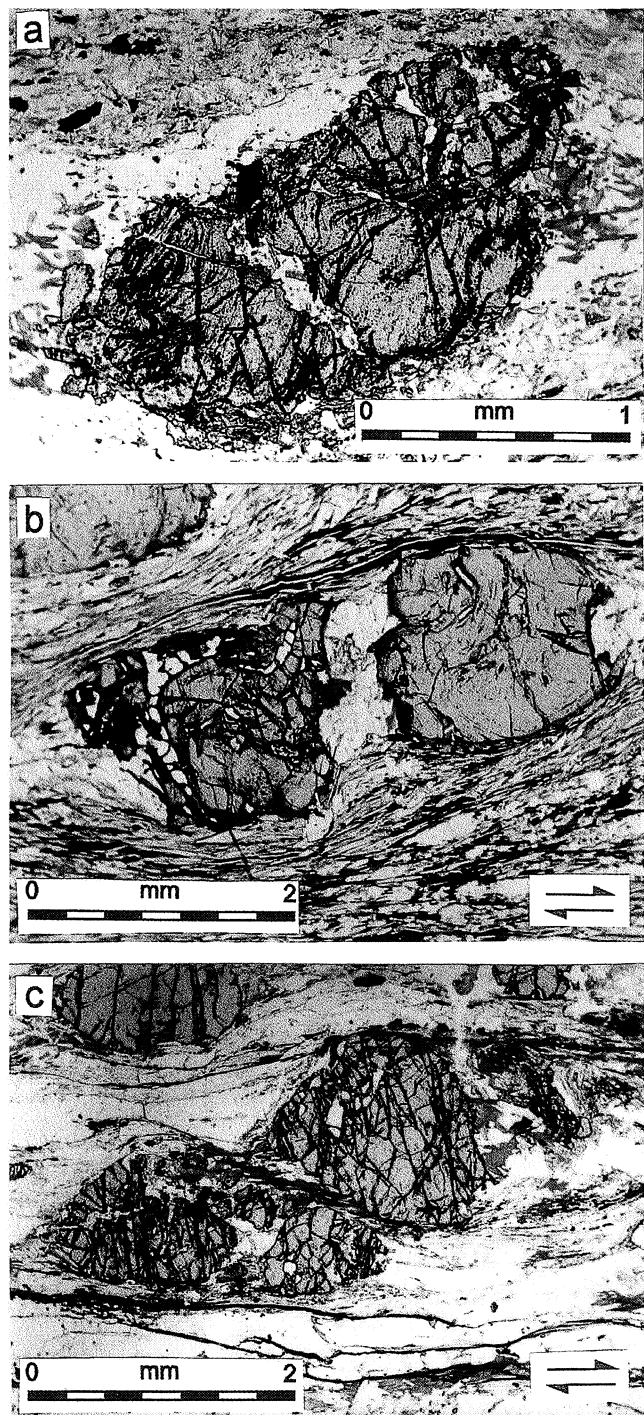


**Fig. 15.** Garnet porphyroclasts subjected to the brittle deformation D<sub>3</sub>. Displaced fragments of broken porphyroclasts indicate a top-to-SW sense of shear in (b) and (c). **a** – small crenulations of the S<sub>1</sub> foliation, developed during the D<sub>2</sub> deformation, are preserved in the broken porphyroblast, **b** – synkinematic quartz and biotite occur between two stretched parts of broken porphyroblast, **c** – synkinematic biotite concentrates along the shear plane cross-cutting the porphyroblast

### Deformation D<sub>3</sub>

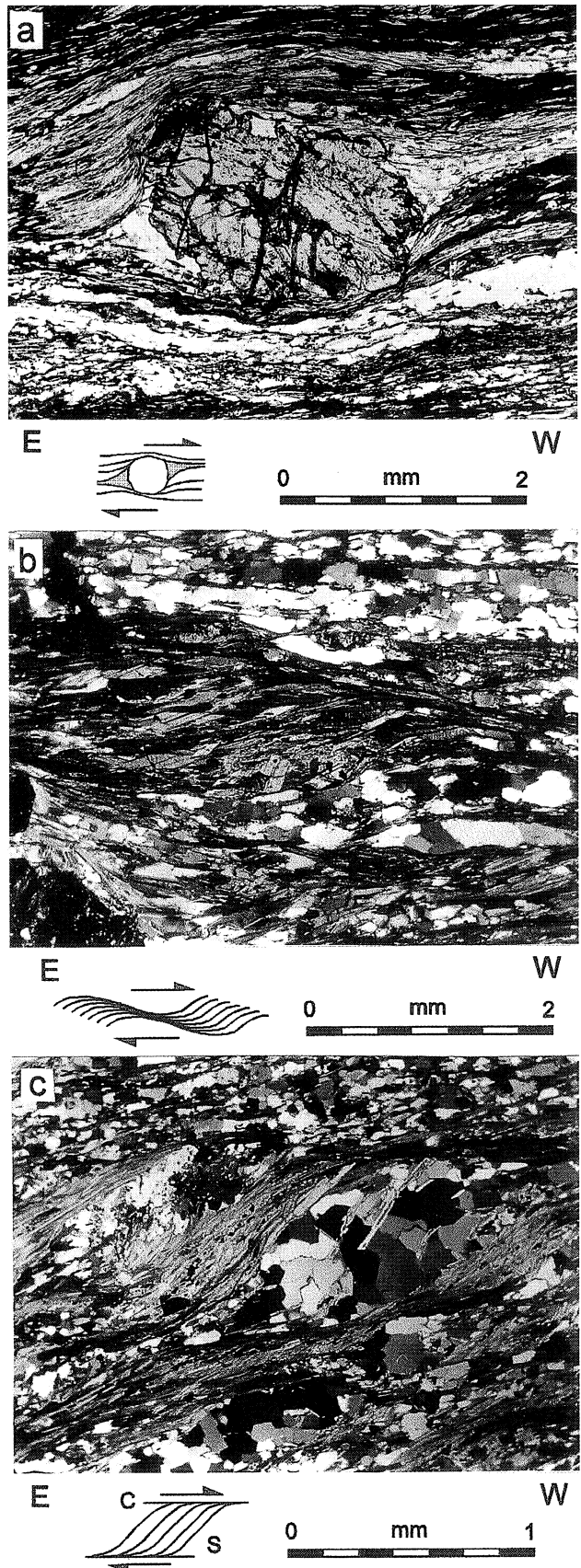
Most of the fine-grained mica schists recorded the effects of non-coaxial shearing along S<sub>3</sub> planes essentially

**Fig. 16.** Examples of kinematic indicators related to the D<sub>3</sub> deformation in the mica schists from the vicinity of Kamieniec Ząbkowicki. In all three cases sense of shear is top-to-SW along the S<sub>2+3</sub> foliation: **a** – asymmetric pressure shadows around garnet porphyroblast in fine-grained mica schist (Kamieniec unit), **b** – extensional crenulation cleavage in fine-grained mica schist (Kamieniec unit), **c** – S-C structure in albite-bearing mica schist (Byczęń unit)

parallel to foliation S<sub>2</sub>. Distinctly asymmetric garnet pressure shadows (Fig. 16a), S-C fabric (Fig. 16c) and extensional crenulation cleavage (Fig. 16b) indicate a top-to-SW or to-WSW sense of shear. The stretching lineation L<sub>3</sub>, defined by micas on the S<sub>2+3</sub> foliation, plunges to the WSW (Fig. 8d, 14b) and is parallel to the lineation L<sub>2</sub>. In general, a contribution of non-coaxial shear to the total strain of the fine-grained mica schists, as expressed by the degree of fabric asymmetry, increases eastwards towards the contact with the albite-bearing schists. In the latter rocks an opposite trend is evident – a westward increase of non-coaxial component towards the boundary with the staurolite and garnet bearing mica schists.

The non-coaxial deformation D<sub>3</sub> has modified the older symmetric fabric of the fine-grained mica schists, developed during the D<sub>2</sub> event (Fig. 15). The foliation S<sub>2+3</sub> was reactivated by non-coaxial shear within D<sub>3</sub> shear zones. Structural observations in the fine-grained schists displaying clearly asymmetric fabric show that some garnet and plagioclase crystals, which had grown during the D<sub>2</sub> event, were subsequently converted into porphyroclasts by the D<sub>3</sub> shearing. These grains are fractured and their fragments displaced along the S<sub>2+3</sub> foliation planes (Fig. 15b, c). At the same time, a reactivation of the S<sub>2+3</sub> planes during the D<sub>3</sub> event led to a complete destruction of the S<sub>1</sub> relics. The only traces of the older foliation S<sub>1</sub> are in these rocks represented by inclusion trails, conserved in the D<sub>2</sub> porphyroblasts. An intense modification of the D<sub>2</sub> fabric in the zones of non-coaxial D<sub>3</sub> shear is indicated by relics of the S<sub>2</sub> crenulation cleavage in pressure shadows of garnet porphyroclasts enveloped by penetrative foliation S<sub>3</sub>. Further evidence for the superimposed D<sub>3</sub> non-coaxial deformation is provided by the presence of microscopic shear zones which developed parallel to the S<sub>2</sub> crenulation cleavage. Relics of crenulated foliation S<sub>1</sub> are still well-visible outside these shear zones whereas they are entirely transposed into a new foliation, S<sub>3</sub>, within zones of the D<sub>3</sub> shear. Superposition of non-coaxial D<sub>3</sub> deformation on the pre-existing crenulation cleavage is also manifested by anastomosing D<sub>3</sub> shear zones enclosing lensoidal microlithons with crenulated relics of S<sub>1</sub>. Foliation planes S<sub>1</sub> are deformed in those places into asymmetrical microfolds of sigmoidal shape.

A characteristic component of both the coarse- and fine-grained varieties of mica schists are andalusite porphyroblasts (Fig. 17). They are lacking only in the albite-bearing mica schists. In the coarse-grained schists, andalusite always forms postkinematic porphyroblasts. They usually contain inclusion trails parallel to the foliation S<sub>2+3</sub> or deformed into small crenulations similar to those which are



visible in the surrounding rock (Fig. 17a). In places, postkinematic andalusite has grown in cracks within broken garnet grains (Fig. 17b). Postkinematic porphyroblasts of andalu-

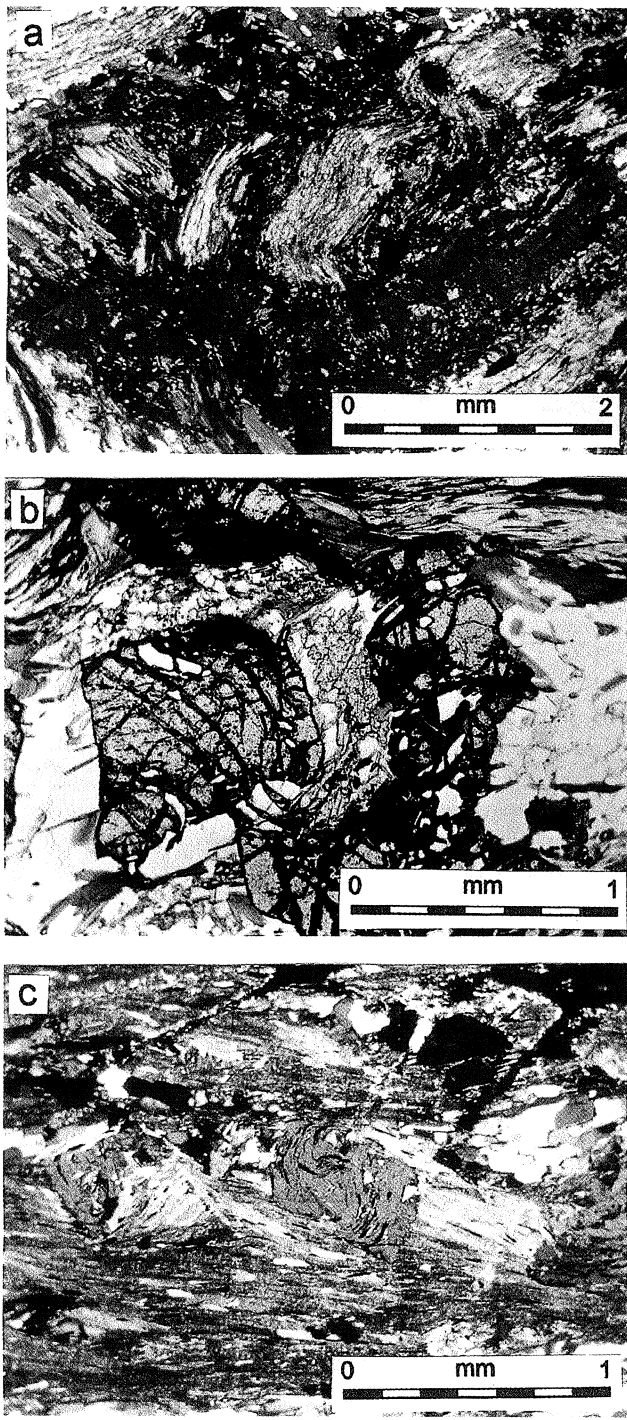


**Fig. 17.** Andalusite in mica schists (Kamieniec unit): **a** – small crenulations of foliation, developed during the D<sub>2</sub> deformation, preserved in the postkinematic andalusite porphyroblast from coarse-grained schists, **b** – postkinematic andalusite in the crack of garnet grain from coarse-grained schists, **c** – spiral inclusion trails in the synkinematic andalusite porphyroblasts developed during the D<sub>3</sub> deformation in fine-grained schists

site are also present in the fine-grained schists showing a symmetric D<sub>2</sub> fabric. On the other hand, synkinematic andalusite crystals occur in the fine-grained mica schists characterised by the asymmetric D<sub>3</sub> fabric (Fig. 17c).

## ANALYSIS OF QUARTZ $\langle c \rangle$ AXIS ORIENTATION

Information provided by quartz  $\langle c \rangle$  axis analysis is consistent with the structural data presented above. Quartz  $\langle c \rangle$  axis patterns obtained in the coarse-grained mica schists from the vicinities of Kamieniec Ząbkowicki (Fig. 18) represent three basic types of scatter: (1) single girdle inclined to foliation, (2) (I) type of crossed girdles (Schmid & Casey, 1986) or small circles centred around the poles to foliation S<sub>1</sub> and (3) isotropic scatter. A single girdle is usually interpreted to be result of the simple shear (Schmid & Casey, 1986). Inclination of the girdle to foliation (Fig. 18a, b) indicates a top-to-E sense of shear. Such kinematics is characteristic of the D<sub>1</sub> deformation responsible for the development of the S<sub>1</sub> foliation. It seems that the D<sub>1</sub> quartz fabric in the coarse-grained schist might partly avoid later modification. (I) type of crossed girdles (Fig. 18c, d) and two small circles patterns (Fig. 18e) indicate a coaxial deformation: pure shear and coaxial flattening, respectively (Schmid & Casey, 1986). Coaxial deformation recorded by quartz fabric in most samples is probably related to the D<sub>2</sub> event and the development of crenulation cleavage S<sub>2</sub>. An isotropic scatter (Fig. 18f) obtained in the well-foliated mica schist suggests post-deformation static recrystallisation.

Quartz  $\langle c \rangle$  axis patterns from the fine-grained mica schists represent two basic types: (1) single girdle inclined to the foliation (Fig. 19a–d) and (2) (I) type of crossed girdles (Fig. 19g–i). Transitional patterns between these two end members were also found (Fig. 19e, f). An inclination of single girdles (Fig. 19a–d) persistently indicates a top-to-SW or top-to-WSW sense of shear. The single girdles probably represent quartz fabric produced by the D<sub>3</sub> simple shear, whereas the crossed girdles show symmetric fabric developed due to the coaxial D<sub>2</sub> event.

Quartz  $\langle c \rangle$  axis patterns obtained in the mica schists from the vicinities of Stolec (Fig. 20) conform to the same rules as those described above, for the schists exposed around Kamieniec Ząbkowicki. Quartz  $\langle c \rangle$  axis diagrams display an entire spectrum of transitional patterns from a single girdle inclined to foliation to (I) type of crossed girdles (Fig. 20). Some diagrams (Fig. 20d, e) show a distinct tendency to scatter along two small circles around the poles to foliation. Quartz  $\langle c \rangle$  axis analysis indicates that total strain of the mica schists from the vicinity of Stolec involved two main components: simple shear and coaxial strain ranging between pure shear and general flattening. Both components are superimposed in various proportions. Some diagrams (Fig. 20a, b) show patterns representative for a strain very close to a simple shear, whereas others (e.g. Fig. 20e) demonstrate almost symmetric scatter typical of pure shear. An inclination of single girdles with respect to the foliation, indicates a top-to-SW sense of simple shear. Therefore, quartz fabric in mica schists from the vicinity of Stolec presumably developed due to superposition of the D<sub>2</sub> coaxial and the D<sub>3</sub> non-coaxial deformations.

Most samples from all varieties of mica schists yielded quartz  $\langle c \rangle$  axis patterns characterised by maxima located near the centre of diagram. Such patterns are usually interpreted to be indicative of deformation under the conditions

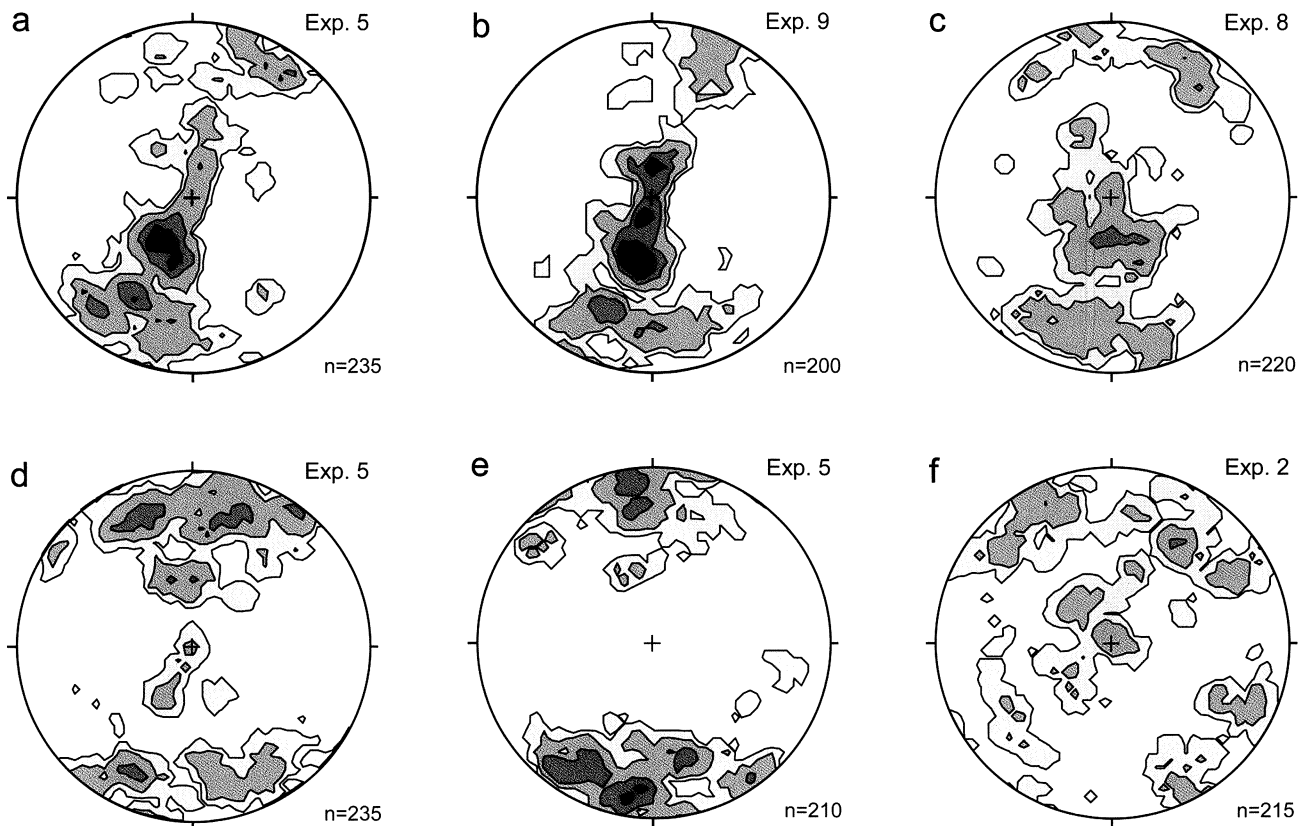


**Fig. 18.** Representative examples of quartz c-axis patterns in coarse-grained mica schists from vicinities of Kamieniec Ząbkowicki. Equal-area net, lower hemisphere. Density contours at 2% intervals. Projection plane is XZ plane of strain ellipsoid. Attitude of foliation corresponds to a plane perpendicular to the figure. Lineation (parallel to X axis of strain ellipsoid) trends parallel to the figure. **a, d, e** – exposure 5; **b** – exposure 9; **c** – exposure 8; **f** – exposure 2

of the upper greenschist or amphibolite facies (Schmid & Casey, 1986). This corollary is confirmed by composition of mineral assemblages which are in the mica schists synkinematic with D<sub>1</sub>–D<sub>3</sub> events.

## DISCUSSION

The effects of the deformation D<sub>1</sub> are preserved in the coarse-grained mica schists. The foliation S<sub>1</sub> represents the main planar structures in these rocks, whereas the lineation L<sub>1</sub> is almost entirely obliterated by younger lineation L<sub>2</sub>. Kinematic indicators suggest that the foliation S<sub>1</sub> was produced by non-coaxial shearing. A restoration of the original direction of shear is difficult due to reorientation of the stretching lineation L<sub>1</sub> on limbs of F<sub>2</sub> folds (Fig. 5c). Assuming that the foliation S<sub>1</sub> had been subhorizontal before the D<sub>2</sub> event, the incipient orientation of L<sub>1</sub> was E–W. If this reasoning is correct, the kinematic indicators recorded a top-to-E sense of shear during the D<sub>1</sub> deformation.

The chemical composition of minerals that define the foliation S<sub>1</sub> in the coarse-grained mica schists, together with the composition of synkinematic garnet porphyroblasts in these rocks, indicate that the deformation D<sub>1</sub> took place under upper amphibolite facies conditions (Józefiak, 1996). The temperatures calculated by Józefiak using garnet-biotite geothermometer (Ferry & Spear, 1978; Hodges & Spear,

1982; Ganguly & Saxena, 1984) are within the range of 570–640°C (Józefiak, 1996). Pressure estimated for the D<sub>1</sub> event using GASP (Hodges & Crowley, 1986; Koziol & Newton, 1988) and GMBP (Hoisch, 1990) geobarometers ranges between 8 and 13 kbars. High magnitude of pressure calculated by Józefiak for the coarse-grained mica schists, which included intercalations of eclogites (Achramowicz *et al.*, 1997), indicated a continuous transition from eclogite to amphibolite facies at the onset of the D<sub>1</sub>.

The foliation S<sub>1</sub> was deformed during the D<sub>2</sub> event by F<sub>2</sub> folds of the NW asymmetry (Fig. 10). Folds facing the dip direction of the main foliation suggest that the whole rock series in the vicinities of Kamieniec Ząbkowicki and Stolec represents the overturned limb of a F<sub>2</sub> megafold. The same is indicated by the cleavage S<sub>2</sub> of shallower attitude than that of foliation S<sub>1</sub> on the steeper, longer limbs of F<sub>2</sub> folds. Kinematic indicators show that the development of the F<sub>2</sub> folds together with their axial cleavage S<sub>2</sub> was accompanied by coaxial deformation. Quartz <c> axis patterns recorded strain in the field of general flattening or close to pure shear. The lineation L<sub>2</sub> was formed due to coaxial stretching and by intersection of the S<sub>1</sub> foliation and the S<sub>2</sub> cleavage. It parallels axes of F<sub>2</sub> folds which trend NE–SW or ENE–WSW.

A transition from the coarse- to fine-grained mica schists is related to the conversion of cleavage S<sub>2</sub> into the main foliation of the rock. The new foliation S<sub>2</sub> is defined

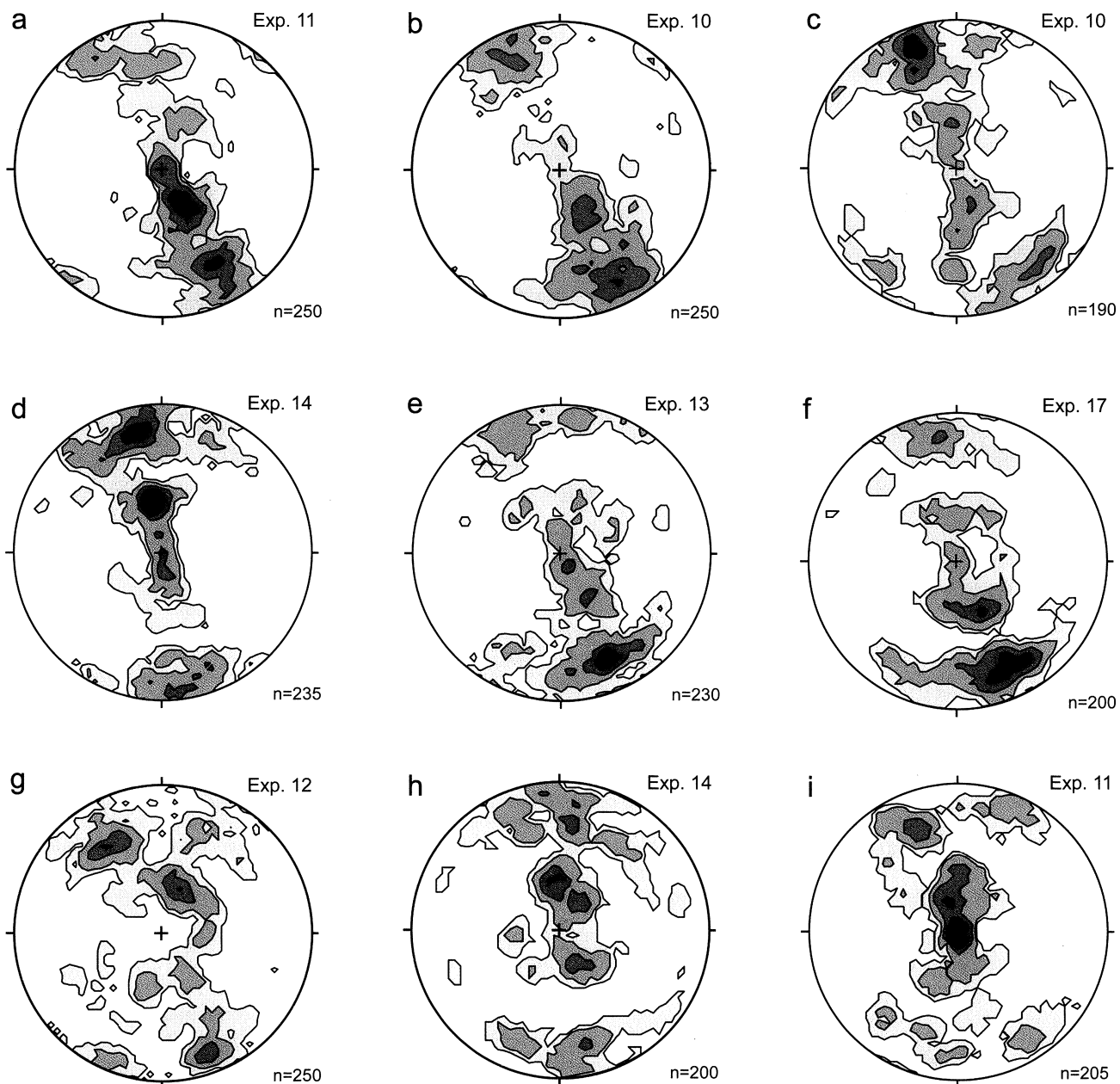


**Fig. 19.** Representative examples of quartz c-axis patterns in fine-grained mica schists from vicinities of Kamieniec Zabkowicki. Equal-area net, lower hemisphere. Density contours at 2% intervals. Projection plane is XZ plane of strain ellipsoid. Attitude of foliation corresponds to a plane perpendicular to the figure. Lineation (parallel to X axis of strain ellipsoid) trends parallel to the figure. **a, i** – exposure 11; **b, c** – exposure 10; **d, h** – exposure 14; **e** – exposure 13; **f** – exposure 17; **g** – exposure 12

by mica and quartz-mica layers developed due to increasing strain. Therefore, the coarse-grained mica schists must represent a less strained zone of the rock sequence which is characterised by the D<sub>1</sub> fabric not obliterated by the D<sub>2</sub> structures. On the contrary, the fine-grained schists were subjected to a relatively higher strain during the D<sub>2</sub> event. Consequently, the differentiation of mica schists into the coarse- and fine-grained varieties reflects variable intensity of the D<sub>2</sub> strain within the same complex. Increasing strain resulted in a more uniform attitude of the foliation S<sub>2</sub> in comparison to that of the S<sub>2</sub> crenulation cleavage.

The chemical composition of minerals synkinematic with reference to the D<sub>2</sub> event, suggests a deformation under

lower amphibolite facies conditions (Józefiak, 1996). The temperatures calculated using the garnet-biotite geothermometer (Ferry & Spear, 1978; Hodges & Spear, 1982; Ganguly & Saxena, 1984) are in the range of 510–540°C, whereas the pressure estimated on the basis of GASP (Hodges & Crowley, 1986; Koziol & Newton, 1988) and GMBP (Hoisch, 1990) geobarometers ranges between 7 to 8.5 kbar (Józefiak, 1996). The chemical zonation of garnet porphyroblasts in the fine-grained schists, except for the albitite-bearing schists, indicates an increase in temperature during the D<sub>2</sub> event.

The deformation D<sub>3</sub> is confined mainly to shear zones, developed in the fine-grained mica schists. These zones are

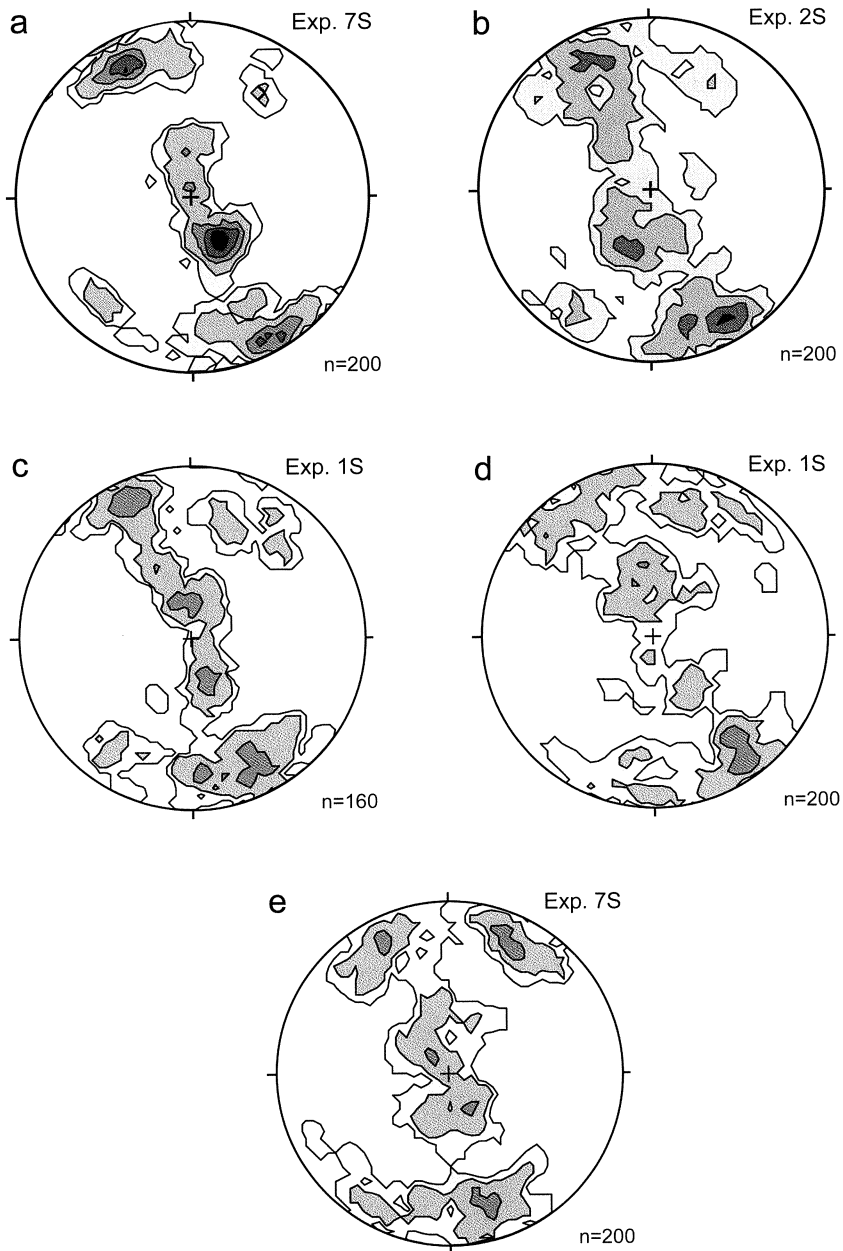


**Fig. 20.** Representative examples of quartz c-axis patterns in mica schists from vicinities of Stolec. Equal-area net, lower hemisphere. Density contours at 2% intervals. Projection plane is XZ plane of strain ellipsoid. Attitude of foliation corresponds to a plane perpendicular to the figure. Lineation (parallel to X axis of strain ellipsoid) trends parallel to the figure. **a, e** – exposure 7S; **b** – exposure 2S; **c, d** – exposure 1S

characterised by a top-to-WSW sense of shear. Deformation D<sub>3</sub> was accompanied by significant decrease of pressure. The occurrence of andalusite indicates decompression from 7–8 kbar during the D<sub>2</sub> to 2–4 kbar during the D<sub>3</sub> deformation. The latter event took place under still relatively high temperature, exceeding 500°C. This suggests very rapid exhumation of the whole rock complex. Only local synkinematic chlorite documents temperature retrogression during the late phase of the D<sub>3</sub> event.

There is a distinct contrast of mineral composition between (1) the coarse- and fine-grained mica schists with staurolite and garnet porphyroblasts and (2) the albite-bear-

ing mica schists. This difference partly reflects the contrast in bulk chemical composition of both rock types (Tab. 2) since the albite-bearing schists are less oversaturated in alumina. On the other hand, the observed difference in mineral composition points to a lower metamorphic grade of albite-bearing schists. During the D<sub>1</sub> event they were metamorphosed under conditions transitional between those of greenschist and amphibolite facies, as indicated by large amount of spessartine component (Spe27) in scarce garnet porphyroclasts. The contrast of metamorphic grades between the two varieties of mica schists, apparent during the D<sub>1</sub> deformation, is less evident during the D<sub>2</sub> and D<sub>3</sub> events. The crystallization of albite porphyroblasts in the plagioclase-rich mica schists during the D<sub>2</sub> deformation could have taken place under the conditions comparable to those calculated for the fine-grained mica schists with staurolite and abundant garnet (510–540°C). The development of albite was possible under temperatures exceeding 500°C, since the relatively high pressure of about 8 kbars enlarged a stability field of this mineral phase. Rapid decompression during the D<sub>3</sub> event probably resulted in the growth of small oligoclase grains (20–24% An) which accompanied albite porphyroblasts in the albite-bearing schists. The presence of oligoclase suggests the temperatures still exceeding 500°C during the D<sub>3</sub> deformation, similarly to the temperatures recorded from other varieties of mica schists.

Two large tectonic units were distinguished in the study area, based on the contrasts in metamorphic grade and lithology difference: the Kamieniec unit (higher grade) and the Byczęń unit (lower grade). The boundary between the two units is located to the west of Byczęń (Fig. 2) and continues northward into the vicinity of Stolec (Fig. 3), west of the Wapienna Hill. This boundary is not directly visible in the field, but exposures of mica schists show-

ing contrasting metamorphic grades occur not further apart from each other than a few tens of metres. Therefore, a tectonic character of the contact is inferred for the distinguished units. The results of preliminary investigations (Leszczyński, 1995) suggest that both the Kamieniec and Byczęń units continue northward to the vicinities of Niemcza (Fig. 1). The majority of rocks of the northern segment of the Kamieniec Metamorphic Complex probably belongs to the Byczęń unit.

The Kamieniec unit crops out to the west of the Byczęń unit, between Kamieniec Ząbkowicki and Byczęń (Fig. 2). The foliation dips generally to the west there (Fig. 14), so

**Table 2**

Representative chemical analyses of mica schists containing staurolite and andalusite and mica schist having albite porphyroblasts

Sample	A1166	F1202	F1208	F1209	F1217	F1243	A1167	F1204	F1221	F1232	F1241	F1247	F1224	L1328	L1333	L1357
	c.g.	c.g.	c.g.	c.g.	c.g.	c.g.	f.g.	f.g.	f.g.	f.g.	f.g.	f.g.	a.f.g.	a.f.g.	a.f.g.	a.f.g.
SiO <sub>2</sub>	69.20	61.63	65.23	56.60	68.23	63.21	62.33	60.96	65.78	65.64	67.02	68.34	65.12	66.63	66.82	68.16
TiO <sub>2</sub>	0.73	0.80	0.60	1.04	0.76	0.89	1.02	0.97	0.71	0.75	0.91	0.68	0.70	0.49	0.54	0.48
Al <sub>2</sub> O <sub>3</sub>	14.71	21.52	15.90	22.59	16.44	18.21	19.05	21.07	17.96	17.33	14.51	14.90	15.47	16.26	16.36	15.72
Fe <sub>2</sub> O <sub>3</sub>	0.03	0.28	1.40	1.83	0.68	1.39	3.87	2.22	0.05	1.71	1.81	3.07	3.84	0.61	0.05	0.67
FeO	2.54	4.68	7.01	5.34	3.77	4.32	2.32	4.10	5.65	4.24	4.06	3.95	2.37	4.28	4.40	3.99
MnO	0.07	0.11	0.22	0.24	0.14	0.09	0.26	0.26	0.34	0.13	0.31	0.40	0.08	0.04	0.04	0.04
MgO	3.78	1.56	1.75	2.08	1.31	1.96	1.67	1.84	1.56	1.43	2.06	1.75	1.64	2.03	1.90	1.82
CaO	1.14	1.11	1.25	0.92	1.24	0.95	0.97	0.78	1.01	0.83	0.80	0.78	1.46	1.62	2.08	1.40
Na <sub>2</sub> O	2.95	0.94	1.16	1.42	1.51	1.25	0.76	0.85	1.20	1.54	1.49	0.95	3.09	2.67	3.49	2.65
K <sub>2</sub> O	2.89	4.22	3.44	4.67	3.52	4.25	3.80	3.82	3.33	4.15	3.74	3.01	3.09	2.94	2.90	3.54
P <sub>2</sub> O <sub>5</sub>	0.15	0.18	0.10	0.10	0.16	0.09	0.09	0.08	0.14	0.11	0.17	0.13	0.17	0.12	0.14	0.11
H <sub>2</sub> O	1.39	2.73	1.59	2.89	1.98	2.57	3.40	2.80	2.04	1.99	3.31	2.32	3.20	2.06	1.08	1.23
total	99.77	99.76	99.65	99.72	99.74	99.18	99.73	99.75	99.77	99.85	100.19	100.28	100.23	99.75	99.80	99.81
Q	32.29	33.51	35.95	23.21	40.28	33.61	40.60	36.22	38.38	35.52	38.65	46.35	31.09	30.75	25.28	31.10
Or	17.41	25.73	20.75	28.53	21.30	26.02	23.38	23.31	20.16	25.09	22.84	18.18	18.84	17.42	17.18	20.97
Ab	25.40	8.19	10.00	12.40	13.06	10.94	6.68	7.41	10.38	13.30	13.00	8.20	26.92	22.65	29.59	22.47
An	4.77	4.47	5.66	4.04	5.23	4.27	4.40	3.46	4.20	3.48	2.96	3.09	6.33	7.27	9.42	6.24
C	5.10	14.23	8.38	14.20	8.45	10.38	12.61	14.75	11.12	9.24	7.18	9.15	4.93	6.04	4.04	5.26
Hy	13.25	11.48	15.80	12.61	8.83	10.74	4.34	9.46	14.00	9.14	10.50	8.89	4.40	11.71	11.99	10.61
en	9.63	4.02	4.46	15.37	3.35	5.07	4.34	4.75	3.99	3.65	5.32	4.47	4.23	5.07	4.74	4.54
fs	3.62	7.46	11.34	7.24	5.48	5.66	0.00	4.71	10.01	5.48	5.19	4.42	0.17	6.64	7.25	6.06
Mt	0.04	0.42	2.07	2.74	1.01	2.09	5.58	3.32	0.07	2.53	2.71	4.54	5.74	0.89	0.07	0.97
Il	1.41	1.57	1.16	2.04	1.48	1.75	2.02	1.90	1.38	1.46	1.79	1.32	1.37	0.93	1.03	0.91
Ap	0.33	0.41	0.22	0.23	0.36	0.20	0.20	0.18	0.31	0.25	0.38	0.29	0.38	0.28	0.32	0.26

Mica schists containing staurolite and andalusite: c.g. – coarse-grained, f.g. – fine-grained, a.f.g. – albite-bearing fine-grained mica schist. Samples L1328, L1333 and L1357 were collected north of Niemcza in the vicinities of Księginięce Wielkie (presented after Leszczyński, 1995).

that the Kamieniec unit probably overlies the Byczęń unit in that area. An opposite situation is encountered in the vicinity of Stolec, where the Byczęń unit is interpreted to overlie the Kamieniec unit, exposed more to the east (Fig. 3). In general, the Kamieniec unit recorded an increase of temperature (D<sub>2</sub> event) and a higher metamorphic grade during the D<sub>2</sub> and D<sub>3</sub> deformations and, thus, probably underlies the Byczęń unit. Such a tectonic sequence, actually observed in the vicinity of Stolec, is interpreted here, as a result of the F<sub>2</sub> folding. On the other hand, the outcrop pattern between Kamieniec Ząbkowicki and Stolec may represent an intersection effect caused by (1) N–S trending brittle normal fault dipping steeply to the east (Behr, 1926; Baraniecki, 1956) or (2) low-angle normal shear-zone dipping to WSW. The latter interpretation, preferred by the present authors, is in agreement with the observed increase in the intensity of D<sub>3</sub> simple shear deformation towards the contact of the Kamieniec and Byczęń units. The simple shear strain

is related to the development of ductile D<sub>3</sub> shear zone occurring at the boundary of both units (Fig. 21). This shear zone is parallel to the foliation S<sub>2+3</sub>, which dips to the WSW at an angle of 20°. A normal-slip top-to-WSE sense of shear, along the L<sub>3</sub> lineation, is defined by numerous kinematic indicators.

A ductile shear zone which represents the boundary of the Kamieniec and Byczęń units to the west of Byczęń, is less inclined than the primary tectonic contact of these both units formed during the D<sub>1</sub> event (Fig. 21c). Therefore, a fragment of the Kamieniec unit is inferred to have been displaced to the WSW on the hanging wall of the normal-slip D<sub>3</sub> shear zone, above the Byczęń unit (Fig. 21b). The horizontal amplitude of this translation inferred from a geological map, probably exceeds 5 km. A later erosional exhumation resulted in exposing the Kamieniec unit on the hanging wall of the D<sub>3</sub> shear zone to the west of Byczęń (Fig. 21b). The primary contact of the Kamieniec and Byczęń units

within its foot wall is now hidden under Cenozoic sediments east of Byczeń (Fig. 21c). The same contact is exposed within the hanging wall more to the north in the vicinities of Stolec (Fig. 21a).

The results of our investigations allow us to update the preliminary interpretation by Mazur & Puziewicz (1995a, b) and by Mazur *et al.* (1995), who considered the L<sub>2</sub> lineation in the mica schists of the Kamieniec Ząbkowicki Metamorphic Complex as a structure produced exclusively by non-coaxial shearing. On the other hand, the present study confirms earlier data of several authors, according to which the D<sub>3</sub> deformation concentrated in low-angle shear zones characterised by a normal top-to-WNW or to-SW sense of shear. Results of our study are in agreement with earlier observations by Dziedzicowa (1985, 1987), who proved that the oldest S<sub>1</sub> foliation in the Kamieniec Metamorphic Complex is very steep and involved into F<sub>2</sub> folds with subhorizontal axial planes. Axial cleavage S<sub>2</sub> of these folds obliterates, in places, the older foliation S<sub>1</sub> and contributes to the formation of the L<sub>2</sub> lineation due to intersection of S<sub>1</sub> and S<sub>2</sub> planes (Dziedzicowa, 1985, 1987). The existence, in the study area, of normal-slip shear zones with a top-to-WNW kinematics and of east-vergent thrusts is confirmed by the work of Achramowicz *et al.* (1997), in spite of different interpretation presented in that paper. Our investigations do not comply, however, with data by Cymerman and Piasecki (1994) who postulated the dominant role of the NE-directed thrusting in the eastern part of the Fore-Sudetic block.

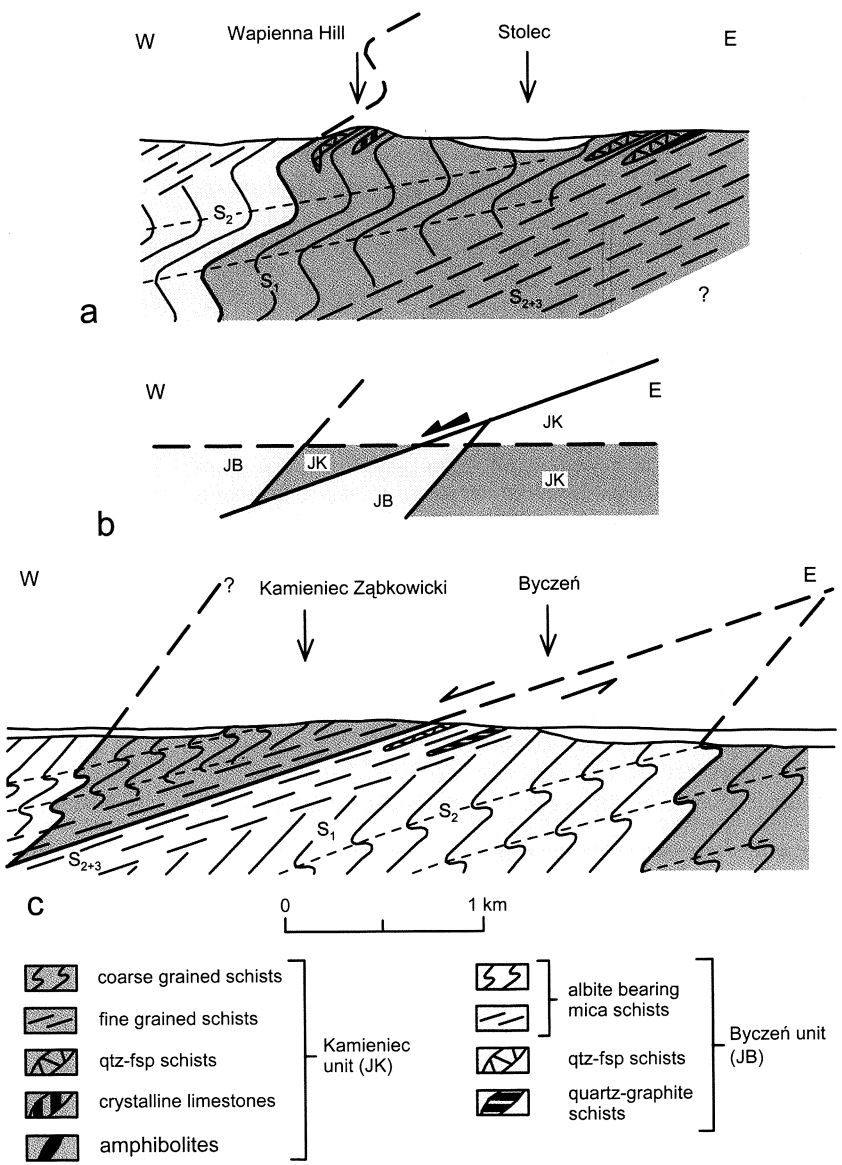


**Fig. 21.** Generalized sections across the contact zone between Kamieniec (JK) and Byczeń (JB) units. **a** – cross-section through the vicinity of Stolec, **b** – schematic diagram explaining the outcrop map-pattern between Kamieniec Ząbkowicki and Byczeń, **c** – cross-section in the vicinity of Kamieniec Ząbkowicki

### TECTONIC EVOLUTION OF METAMORPHIC SERIES BETWEEN THE GÓRY SOWIE AND NIEDZWIEDŹ MASSIFS

The observations from southern part of the Kamieniec Ząbkowicki Metamorphic Complex, complete earlier data from the Niemcza Zone and the Doboszowice Metamorphic Complex (Mazur & Puziewicz, 1995a, b; Mazur *et al.*, 1995; Mazur *et al.*, 1997; Puziewicz & Rudolf, 1998; Puziewicz *et al.*, 1998). They allow us to formulate the preliminary hypothesis explaining the structure and evolution of the metamorphic series between the Góry Sowie Massif and Niedźwiedź Massif (Fig. 22). The deformation D<sub>1</sub>, whose effects are preserved in the coarse-grained mica schists, is equivalent to the deformation described as D<sub>1</sub> by Mazur & Puziewicz (1995b) in the Chałupki paragneiss (Fig. 22). The

D<sub>1</sub> deformation in both areas took place under retrogression of metamorphism from the upper to lower amphibolite facies and was probably related to a top-to-E shearing. On the other hand, the coaxial D<sub>2</sub> deformation of mica schists is equivalent to the deformation recorded by the Doboszowice orthogneiss (Fig. 22). This granite intrusion, recently dated at ca. 380 Ma (A. Kröner – pers. com.), was transformed into an orthogneiss due to deformation comprising mainly a coaxial component. The significance of non-rotational strain is additionally documented by lately published quartz <c> axis analyses (Czapliński *et al.*, 1996; Bartz, 1997). The deformation of the Doboszowice orthogneiss included as well, a component of a top-to-NE simple shear (Mazur & Puziewicz, 1995b). In contrast, no effect of this non-coaxial D<sub>2</sub> shear is recorded in mica schists from vicinities of Kamieniec Ząbkowicki. Apart from fine-grained mica schists, the

results of the D<sub>3</sub> event are also recorded by the Lipniki late tectonic granite. The Lipniki intrusion was deformed in a low-angle normal shear zone characterised by a top-to-WSW sense of shear (Mazur *et al.*, 1997). The D<sub>3</sub> event involved, as well, the development of the Niemcza Zone which represented a sinistral strike-slip shear zone of regional scale (Mazur & Puziewicz, 1995a, b). A sinistral shear along the subvertical Niemcza Zone was accompanied, according to Mazur and Puziewicz (1995a, b), by a top-to-WSW or top-to-SW normal shear on the shallow dipping S<sub>2+3</sub> foliation in the mica schists from southern part of the Kamieniec Ząbkowicki Complex.

Our data indicate that the mica schists of the Kamieniec Ząbkowicki Metamorphic Complex are exposed on the shorter limb of an asymmetric F<sub>2</sub> megafold. On the other hand, the Chałupki paragneiss is exposed on the longer limb of the same fold (Fig. 23). The mesofolds in the paragneiss show SE asymmetry, i. e. opposite to the asymmetry of mesofolds in the mica schists. Their axial cleavage, S<sub>2</sub>, is steeper than the foliation S<sub>1</sub> (Mazur & Puziewicz, 1995b; Mazur *et al.*, 1995). Both limbs of the F<sub>2</sub> megafold define an asymmetric synform, overturned to the SE, with a NE–SW trending subhorizontal axis (Fig. 23). In the hinge of this synform there occur the Doboszowice orthogneiss, preliminary interpreted as a syntectonic intrusion (Mazur & Puziewicz, 1995b). In the west, the strike-slip Niemcza Zone

separates the overturned limb of the F<sub>2</sub> megafold from the Góry Sowie Massif (Fig. 23).

The reconstruction of the F<sub>2</sub> synform allows the structural position to be determined for the three tectonic units exposed in the study area (Fig. 22). From bottom to top, these are: (1) Byczeń unit, (2) Kamieniec unit and (3) Chałupki unit (paragneisses and amphibolites). They represent a pre-D<sub>2</sub> stack of thrust sheets characterised by tectonic inversion of metamorphic grade. The two upper thrust sheets (Kamieniec and Chałupki units) represent a higher metamorphic grade (upper amphibolite facies) than the lowermost, Byczeń, unit (lower amphibolite facies). On the other hand, the Kamieniec and Chałupki units differ in the maximum values of temperatures recorded during the early phase of metamorphism. The uppermost, Chałupki unit comprises granulites metamorphosed under the temperature reaching up to 920 °C (Achramowicz *et al.*, 1995), whereas the lower, Kamieniec unit contains eclogites metamorphosed under temperature of 575 °C (Achramowicz *et al.*, 1997). At the base of the distinguished thrust sequence the main thrust (Paczków thrust) occurs, which separates it from the underlying metabasites of the Niedźwiedź massif (Fig. 23).

The development of the described nappe pile during the D<sub>1</sub> event was coeval with the thrusting of the West Sudetes over the East Sudetes. The direction of tectonic transport

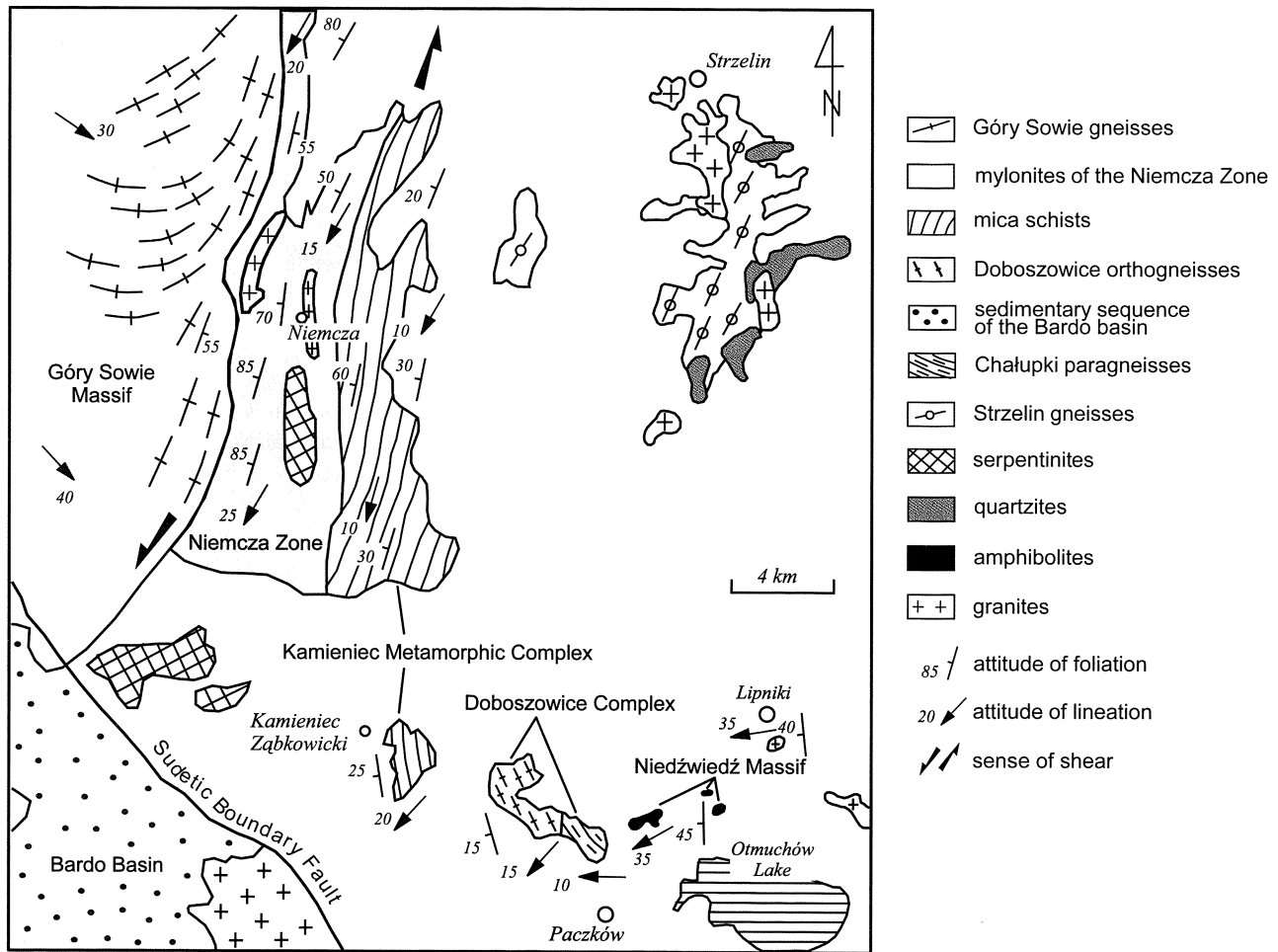
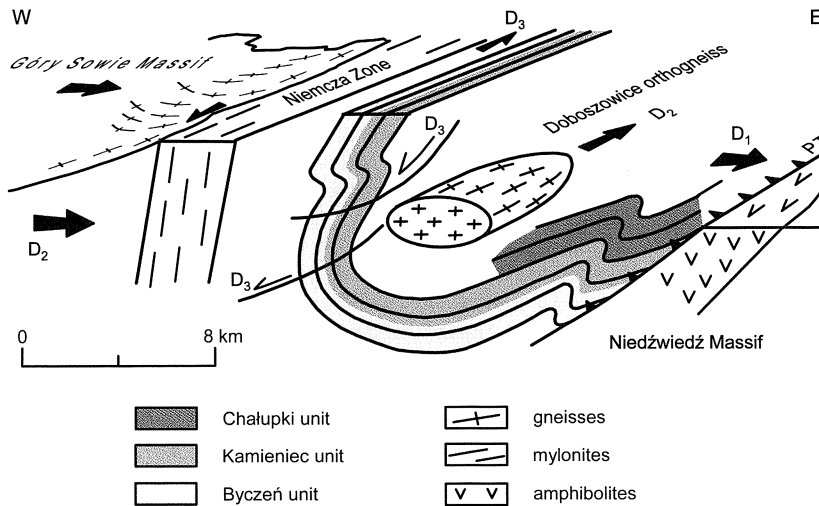


Fig. 22. Simplified tectonic map of metamorphic complexes cropping out between the Góry Sowie Massif and the Niedźwiedź Massif



**Fig. 23.** Schematic block diagram showing the structural geometry of metamorphic complexes between the Góry Sowie Massif and the Niedźwiedź Massif. Chałupki, Kamieniec and Byczeń units are separated by overthrusts (here omitted for sake of simplicity). PT – Paczków overthrust

was probably towards the east, in agreement with the classical interpretation of Suess (1912). An eastward direction of the overthrusting is indicated by E–W orientation of the stretching lineation L<sub>1</sub> and by consistent east-verging asymmetry of kinematic indicators in both normal and inverted limbs of the NE–SW trending megasynform F<sub>2</sub>. The kinematic indicators both in the Chałupki paragneiss (Mazur & Puziewicz, 1995b; Puziewicz *et al.*, 1998) and in the coarse-grained mica schists of the Kamieniec unit suggest a persistent top-to-E sense of shear. This implies that the direction of tectonic transport during the D<sub>1</sub> event was probably oblique at high angle or perpendicular to the axis of the later F<sub>2</sub> synform.

The folding and coaxial shortening during the D<sub>2</sub> event probably represented a continuation of E–W-directed contraction, which had previously given rise to the nappe stacking. The highest strain was imposed, during the D<sub>2</sub> event, on a shorter limb of the F<sub>2</sub> synform. It was subjected to progressive coaxial shortening which produced the crenulation cleavage and foliation S<sub>2</sub>. High strain concentrated, as well, in the syn-tectonic Doboszowice intrusion due to its low competence. The Doboszowice granite was transformed into the orthogneiss as a result of deformation comprising coaxial NW–SE shortening and a top-to-NE non-coaxial shearing. The significance of the latter component cannot be estimated in the study area.

The deformation D<sub>3</sub> was related to WSW-directed extensional collapse of a regional extent. A similar deformation has been recently described in the Jesenik Massif (Czermman, 1993; Chab *et al.*, 1994; Schulmann *et al.*, 1995). The extensional collapse was accompanied by the development of the subvertical strike-slip Niemcza Shear Zone along the eastern margin of the Góry Sowie Massif (Mazur & Puziewicz, 1995). Low-angle normal-slip D<sub>3</sub> shear zones developed in the rocks subjected to the high strain during the D<sub>2</sub> event (fine-grained mica schists) or in low-competence rocks (late tectonic Lipniki granite). The transition from co-

axial shortening to non-coaxial WSW-directed extensional collapse reflects, in our opinion, a response of the rocks to increasing deformation in high strained zones.

The extensional collapse resulted in rapid decompression which was recorded by andalusite growth. In the D<sub>3</sub> shear zones the andalusite is synkinematic, whereas in rocks subjected only to coaxial strain it is postkinematic. This indicates that rock volumes in which the deformation had ceased after the D<sub>2</sub> coaxial flattening subsequently underwent only passive displacement along the D<sub>3</sub> shear zones.

Timing the main deformation events is still poorly constrained. The approximate age of the deformation D<sub>2</sub> probably represents the age of the Doboszowice orthogneiss considered to be a syntectonic intrusion (Mazur & Puziewicz, 1995; Puziewicz & Rudolf, 1995). The magmatic protolith of the Doboszowice gneiss has been recently dated at 379 ± 1 Ma (A. Kröner – pers. com.), using U–Pb evaporation method on single zircons. The deformation D<sub>1</sub> must have predated the emplacement the Doboszowice intrusion so that it was probably Middle Devonian in age. On the other hand, the age of the extensional collapse D<sub>3</sub> is constrained in a wide time interval by the age of the D<sub>2</sub> event (ca. 380 Ma) and the age of the late- to post-tectonic granite from the Niemcza Zone dated at ca. 340 Ma (Oliver *et al.*, 1993).

## CONCLUSIONS

The metamorphic complexes exposed between the Góry Sowie Massif and the Niedźwiedź Massif display a nappe structure. Three tectonic units (Chałupki, Kamieniec and Byczeń units) of different metamorphic history were subjected to ductile overthrust towards the east during the D<sub>1</sub> event. A penetrative foliation S<sub>1</sub> was formed parallel to thrust planes and a stretching lineation L<sub>1</sub> developed parallel to the thrust direction. Subsequent folding and coaxial shortening during the D<sub>2</sub> event produced lineation L<sub>2</sub> trending NE–SW, that represented a dominant linear structure in the area. At the same time subhorizontal axial cleavage of F<sub>2</sub> folds was transposed, in places, into a new penetrative foliation S<sub>2</sub> overprinting the older foliation S<sub>1</sub>. The deformation D<sub>2</sub> was presumably accompanied by a syntectonic granite intrusion, subsequently transformed into the Doboszowice orthogneiss. The eventual tectonic event D<sub>3</sub> involved WSW-directed extensional collapse recorded by the development of low-angle normal-slip shear zones. The sinistral strike-slip Niemcza Shear Zone formed along the eastern margin of the Góry Sowie Massif during the same D<sub>3</sub> event.

### Acknowledgements

The authors gratefully appreciate a fruitful discussion with Jacek Puziewicz and Paweł Aleksandrowski. The anonymous referees are thanked for their helpful comments. The authors' work was supported by grants 2022/W/ING/97-29 and 2158/W/ING/97 provided by University of Wrocław. Dariusz Józefiak acknowledges a scholarship from the Foundation for Polish Science.

### REFERENCES

- Achramowicz, S., 1994. Rekonstrukcja paleonaprężeń związanych z intruzją hercyńskich granitoidów masywu Strzelina na podstawie analizy struktur dylatacyjnego odkształcania odśrodkowego. Paleostresses in the country rocks of the Strzelin granitoids from the analysis of dilational centrifugal structures, SW Poland. *Ann. Soc. Geol. Pol.* 63: 265–332.
- Achramowicz, S., Muszyński, A. & Schliestedt, M., 1994. New eclogites in the Sudetes Mts. *Mitt. Österr. Miner. Ges.*, 139: 15–16.
- Achramowicz, S., Muszyński, A. & Schliestedt, M., 1995. Wskaźniki wysokotemperaturowej deformacji gnejsów z Doboszowic. (in Polish) *P. T. Min.-Prace specjalne*, Zeszyt 6: 18–20.
- Achramowicz, S., Muszyński, A. & Schliestedt, M., 1997. The northeasternmost eclogite occurrence in the Saxothuringian Zone, West Sudetes (Poland). *Chem. Erde*, 57: 51–61.
- Badura, J., 1979. Szczegółowa mapa geologiczna Sudetów 1:25 000. Arkusz Stolec. Wydawnictwa Geologiczne, Warszawa.
- Badura, J. & Dziemiańczuk, E., 1981. Szczegółowa mapa geologiczna Sudetów 1:25 000. Arkusz Ząbkowice Śląskie. Wydawnictwa Geologiczne, Warszawa.
- Baraniecki, L., 1956. Szczegółowa mapa geologiczna Sudetów 1:25 000. Arkusz Kamieniec Ząbkowicki. Wydawnictwa geologiczne, Warszawa.
- Bartz, W., 1997. Deformacja ortognejsów z Doboszowic w świetle badań uprzedzielającej orientacji krystalograficznej kwarcu. (in Polish) *P. T. Min.-Prace specjalne*, Zeszyt 9: 9–12.
- Bederke, E., 1929. Die Grenze von Ost- und Westsudeten und ihre Bedeutung für die Einordnung der Sudeten in den Gebirgsbau Mitteleuropas. *Geol. Rundsch.*, 20: 186–205.
- Behr, J., 1926. Geologische Karte von Preußen und benachbarten deutschen Ländern. Blatt Camenz. Preuß. Geolog. Land., Berlin.
- Bell, T. H., Rubenach, M. J. & Fleming, P. D., 1986. Porphyroblast nucleation, growth and dissolution in regional metamorphic rocks as a function of deformation partitioning during foliation development. *Jour. Metamorphic Geol.*, 4, p. 37–67.
- Cháb, J., Mixa, P., Vanecek, M. & Žácek V., 1994. Evidence of an extensional tectonics in the NW of the Hrubý Jeseník Mts. (the Bohemian Massif, Central Europe). *Vestnik Českého geol. ustavu*, 63(3): 7–15.
- Cymerman, Z., 1986. Sekwencja deformacji skał metamorficznych z otworu wiertniczego Niedźwiedź IG-2. Sequence of deformations of metamorphic rocks in the borehole Niedźwiedź IG-2 (Lower Silesia). (in Polish, English summary) *Kwart. Geol.*, 30(2): 157–186.
- Cymerman, Z., 1991. Sekwencja deformacji tektonicznych w skałach metamorficznych z otworów wiertniczych Odra 1, 2, 3, 4, 5/I, 5/II (północno-zachodnia część Opolszczyzny). Sequence of tectonic deformations within metamorphic rocks from the boreholes Odra 1, 2, 3, 4, 5/I and 5/II (north western part of the Opole Region). (in Polish, English summary) *Biul. Państw. Inst. Geol.*, 367: 105–133.
- Cymerman, Z., 1993. Czy w Sudetach istnieje nasunięcie ramzowskie? Does the Ramzova thrust exist in the Sudetes? (in Polish, English summary) *Prz. Geol.*, 41(10): 700–706.
- Cymerman, Z. & Jerzmański, J., 1987. Metamorfik wschodniej części bloku przedsudeckiego w okolicy Niedźwiedzia koło Ziębic. Metamorphic rocks of the eastern part of the Fore-Sudetic Block in the region of Niedźwiedź, near Ziębice. (in Polish, English summary) *Kwart. Geol.*, 31(2/3): 239–262.
- Cymerman, Z. & Piasecki, M. A. J., 1994. The terrane concept in the Sudetes, Bohemian Massif. *Kwart. Geol.*, 38(2): 191–210.
- Czapliński, W., Achramowicz, S., Lopez A. L., Pacholska, A. & Żelaźniewicz, A., 1996. Major shear zones in the west Sudetes from quartz microfabric data. In: Abstracts of Europrobe-TESZ Workshop, Książ, 11–17.04.1996.
- Dziedzicowa, H., 1966. Seria łupków krystalicznych na wschód od strefy Niemczy w świetle nowych badań. The schists series east of the Niemcza Zone in the light of new investigations. (in Polish, English summary) W: Z geologii Ziemi Zachodnich, J. Oberc, red., Wrocław: 101–118.
- Dziedzicowa, H., 1973. Mineral parageneses in metamorphic bentonite deposits within the Fore-Sudetic Block. *Bull. Acad. Pol. Sci., Sér. Sci. de la Terre*, 21(2): 99–109.
- Dziedzicowa, H., 1975. Rozwój i sekwenca deformacji w strefie łupków kamieniecko-niemczańskich. (in Polish) Przew. XLVII Zjazdu Pol. Tow. Geol., Świdnica, XXX lat Geologii Polskiej na Dolnym Śląsku, Warszawa.
- Dziedzicowa, H., 1985. Variscan rejuvenation of the Precambrian gneisses along the eastern margin of the Góry Sowie massif, Fore-Sudetic Block. *Krystalinikum*, 18: 7–27.
- Dziedzicowa, H., 1987. Rozwój strukturalny i metamorfizm we wschodnim obrzeżeniu gnejsów Góra Sowich. Structural development and metamorphism in the region east of the Góry Sowie gneissic massif. (in Polish, English summary) *Acta Univ. Wratisl. 788, Prace Geol. Mineral.*, 10: 221–247.
- Ferry, J. M. & Spear, F. S., 1978. Experimental calibration of the partitioning of Fe and Mg between biotite and garnet. *Contrib. Mineral. Petrol.*, 66: 113–117.
- Fritz, H. & Neubauer, F., 1993. Kinematics of crustal stacking and dispersion in the south-eastern Bohemian Massif. *Geol. Rundsch.*, 82: 556–565.
- Ganguly, J. & Saxena, S. K., 1984. Mixing properties of aluminosilicate garnets: constraints from natural and experimental data, and application to geothermo-barometry. *Am. Mineral.*, 69: 88–97.
- Gaździk, J., 1957. Szczegółowa mapa geologiczna Sudetów 1:25 000. Arkusz Przyłęk. Wydawnictwa Geologiczne, Warszawa.
- Hodges, K. V. & Crowley, P. D., 1985. Error estimation and empirical geothermobarometry for pelitic system. *Am. Mineral.*, 70: 702–709.
- Hodges, K. V. & Spear, F. S., 1982. Geothermometry, geobarometry and the  $\text{Al}_2\text{SiO}_5$  triple point at Mt. Moosilauke, New Hampshire. *Am. Mineral.*, 67: 1118–1134.
- Hoisch, T. D., 1990. Empirical calibration of six geobarometers for the mineral assemblage quartz + muscovite + biotite + plagioclase + garnet. *Contrib. Mineral. Petrol.*, 104: 225–234.
- Józefiak, D., 1994. Nowe dane o łupkach lyszczykowych okolic Kamieńca Ząbkowickiego (Dolny Śląsk). (in Polish) *P. T. Min.-Prace specjalne*, Zeszyt 5: 116–118.
- Józefiak, D., 1996. Warunki metamorfizmu łupków lyszczykowych okolic Kamieńca Ząbkowickiego. (in Polish) *P. T. Min.-Prace specjalne*, Zeszyt 7: 54–56.
- Kozioł, A. M. & Newton, R. C., 1988. Redetermination of the garnet-plagioclase- $\text{Al}_2\text{SiO}_5$ -quartz geobarometer. *Am. Mineral.*, 73: 216–223.
- Leszczyński, R., 1992. Petrografia skał krystalicznych okolic

- Księgnic Wielkich. Maszynopis pracy magisterskiej, (in Polish) Instytut Nauk Geologicznych Uniwersytetu Wrocławskiego, 81 s.
- Matte, Ph., Maluski, H., Rajlich, P. & Franke, W., 1990. Terrane boundaries in the Bohemian Massif: Result of large-scale Variscan shearing. *Tectonophysics*, 177: 151–170.
- Mazur, S. & Puziewicz, J., 1995a. Deformacja i metamorfizm serii skalnych na wschód od bloku sowiogórskiego – nowe dane i interpretacje. Deformation and metamorphism of rock series east of the Góry Sowie Block – new data and interpretations. (in Polish, English summary) *Prz. Geol.*, 43: 786–793.
- Mazur, S. & Puziewicz, J., 1995b. Mylonity strefy Niemczy. Mylonites of the Niemcza Fault Zone. (in Polish, English summary) *Ann. Soc. Geol. Polon.*, 64: 23–52.
- Mazur, S., Puziewicz, J. & Józefiak, D., 1995. Strefa Niemczy – regionalna strefa ścinania pomiędzy obszarami o odmiennie ewolucji strukturalno-metamorficznej. The Niemcza Zone – a regional-scale shear zone between two areas of contrasting tectono-metamorphic evolution. (in Polish, English summary) *Przew. LXVI Zjazdu PTG*: 221–240.
- Mazur, S., Puziewicz, J. & Szczepański, J., 1997. Zdeformowane granity z Lipnik na bloku przedsudeckim: zapis waryscyjskiej ekstensji w strefie granicznej zachodnich i wschodnich Sudetów. Deformed granites from Lipniki (Fore-Sudetic Block): record of variscan extension in the West/East Sudetes boundary zone. (in Polish, English summary) *Prz. Geol.*, 45 (3): 290–294.
- Morris, A. P., 1982. Competing deformation mechanisms and slaty cleavage in deformed quartzose metasediments. *J. Geol. Soc. London*, 138: 455–462.
- Nicolas, A. & Poirier, J. P., 1976. Crystalline plasticity and solid state flow in metamorphic rocks. Wiley, London, 444 s.
- Nowak, I., 1995. Historia tektonometamorficzna łupków lyszczykowych okolic Kamieńca Ząbkowickiego. (in Polish) *P. T. Min.- Prace specjalne, Zeszyt 6*: 74–76.
- Nowak, I., 1998. P-T-d path for mica schists associated with eclogites in the Fore-Sudetic Block, SW Poland. *Acta Universitatis Carolinae, Abstracts Volume 42(2)*: 310–311.
- Oberc, J., 1968. Granica między strukturą zachodnio- i wschodniosudecką. (in Polish, English summary) *Ann. Soc. Geol. Polon.*, 38(2/3): 203–217.
- Oliver, G. J. H., Corfu, F., & Krogh, T. E., 1993. U-Pb ages from SW Poland: evidence for a Caledonian suture zone between Baltica and Gondwana. *J. Geol. Soc. London*, 150: 355–369.
- Puziewicz, J. & Rudolf, N., 1998. Petrografia i geneza leukokratycznych gnejsów dwułyszczykowych metamorfiku Doboszowic. Petrology and origin of the leucocratic two-mica gneisses from the Doboszowice metamorphic unit. (in Polish, English summary) *Arch. Miner.*, 51: 181–212.
- Puziewicz, J., Mazur, S. & Papiewska, C., 1998. Petrografia i geneza gnejsów dwułyszczykowych metamorfiku Doboszowic (Dolny Śląsk) i towarzyszących im amfibolitów. Petrology and origin of the two-mica gneisses and concurrent amphibolites from the Doboszowice metamorphic unit. (in Polish, English summary) *Arch. Miner.* – w druku.
- Schmid, S. & Casey, M., 1986. Complete fabric analysis of some commonly observed quartz c-axis patterns. [In:] Hobbs B. E. & Heard H. C. (eds) Mineral and Rock Deformation: Laboratory Studies – The Paterson Volume. Am. Geophysical Union, Geophysical Monograph, 36: 263–286.
- Schulmann, K., Ledru, P., Autran, A., Melka, R., Lardeaux, J. M., Urban, M. & Lobkowicz, M., 1991. Evolution of nappes in the eastern margin of the Bohemian Massif: A kinematic interpretation. *Geol. Rundsch.*, 80: 73–92.
- Schulmann, K., Gayer, R. & Cháb, J., 1995. Silesian domain. Thermal and Mechanical Interactions in Deep Seated Rocks, Excursion Guide – Post-Conference Excursion, 1-4.10.1995, Czech Republic.
- Shelley, D., 1982. Quartz and sheet silicate preferred orientation of low symmetry. Pikkiruna schist, New Zealand. *Tectonophysics*, 83: 309–327.
- Skácel, J., 1989. Hranice Lugika a Silezika (středních a východních Sudet). *Acta Univ. Wratisl. 1113, Prace Geol. Mineral.*, 17: 45–55.
- Starkey, J. & Cutforth, C., 1978. A demonstration of the interdependence of the degree of quartz-preferred orientation and quartz content of deformed rocks. *Can. J. Earth Sci.*, 15: 841–843.
- Suess, F. E., 1912. Die moravischen Fenster und ihre Beziehung zum Grundgebirge des Hohen Gesenke. *Denkschr. kk Akad. Wiss. math-naturwiss Kl* 83: 541–631.
- Suess, F. E., 1926. Intrusionstektonik und Wandertektonik im varistischen Gebirge. Borntraeger, Berlin: 1–268.
- Walniuk, D. M. & Morris, A. P., 1985. Quartz deformation mechanisms in metasediments from Prins Karls Foreland, Svalbard. *Tectonophysics*, 115: 87–100.

## Streszczenie

### DEFORMACJA W ŁUPKACH ŁYSZCZYKOWYCH Z OKOLIC KAMIEŃCA ZĄBKOWICKIEGO NA BLOKU PRZEDSUDECKIM: WARYSCYJSKA TEKTONIKA PŁASZCZOWINOWA I KOLAPS EKSTENSYJNY

Stanisław Mazur & Dariusz Józefiak

## WSTĘP

Charakter i następstwo deformacji we wschodniej części bloku przedsudeckiego wciąż pozostają przedmiotem wzajemnie sprzecznych interpretacji (Dziedzicowa, 1985, 1987; Cymerman & Jerzmański, 1987; Cymerman & Piasecki, 1994; Achramowicz, 1994; Mazur & Puziewicz, 1995a; Nowak, 1995). Z myślą o dostarczeniu nowych danych na temat historii deformacji wschodniej części bloku przedsudeckiego prowadziliśmy badania w łupkach lyszczykowych z okolic Kamieńca Ząbkowickiego (Fig. 1). Nowe informacje uzyskane w efekcie przeprowadzonych badań pozwoliły sformułować wstępną hipotezę objaśniającą ewolucję tektoniczną serii krystalicznych pomiędzy blokiem sowiogórskim a masywem amfibolitowym Niedźwiedzia (Fig. 1).

Na wschód od strefy Niemczy i bloku gnejsowego Góra Sowich łupki lyszczykowe tworzą południkowo wydłużoną wychodnię (Fig. 1). Jest ona określana w tej pracy mianem metamorfiku Kamieńca Ząbkowickiego. Północna część metamorfiku przylega bezpośrednio od wschodu do strefy Niemczy, podczas gdy część południowa tworzy izolowaną wychodnię w okolicach Kamieńca Ząbkowickiego. Łupki lyszczykowe zawierają wkładki łupków kwarcowo-skaleniowych i marmurów oraz, występujące podrzędnie, soczewki łupków kwarcowo-grafitowych, łupków amfibolowych i eklogitów (Fig. 2, 3).

Penetratywna foliacja w metamorfiku Kamieńca zapada pod zmiennym kątem ku SW, W i NW. Upad foliacji zwiększa się ku zachodowi w strefie kontaktu północnej części metamorfiku ze strefą Niemczy (Mazur & Puziewicz, 1995b). Główna lineacja ma w przybliżeniu stałą orientację, zanurzając się pod niewielkim kątem ku SW i SSW.

Mazur i Puziewicz (1995a, b) oraz Mazur *et al.* (1995) opisują trzy etapy deformacji D<sub>1</sub>, D<sub>2</sub> i D<sub>3</sub> w seriach skalnych położonych na wschód od bloku sowiogórskiego. Etapy D<sub>1</sub> i D<sub>2</sub> są ich zdaniem związane z nasuwaniem płaszczowin, odpowiednio, ku E i NE w warunkach facji amfibolitowej. Odpowiadają one głównym deformacjom kontrakcyjnym w obrębie wschodniej strefy krawędziowej masywu czeskiego związanych z nasuwaniami Sudetów zachodnich na Sudety wschodnie. Etap D<sub>3</sub> był natomiast efektem regionalnej ekstensji zaznaczającej się po fazie tworzenia nasunięć. Struktury powstałe w etapie D<sub>3</sub> wskazują na ścinanie o zwrocie lewoskrętno-przesuwczym, w strefach o stromej foliacji, lub o zwrocie "strop-ku-SW" w obszarach o foliacji subhoryzontalnej (Mazur & Puziewicz, 1995a, b; Mazur *et al.*, 1995).

## LITOLOGIA I PETROGRAFIA

Łupki lyszczykowe z okolic Kamieńca Ząbkowickiego (Fig. 2; odsł. 1–14) są łupkami kwarcowo-muskowitowymi z biotytom, granatem, oligoklazem, andaluzytem, staurolitem i chlorytem. Do minerałów akcesorycznych należą turmalin, apatyt, cyrkon, allanit, rutyl i ilmenit. Wśród łupków występuje zróżnicowane na dwie odmiany strukturalne: grubo- i drobnoblastyczną (Józefiak, 1995).

Łupki drobnoblastyczne (odsł. 10–14) charakteryzują się występowaniem naprzemianległych lamin kwarcowo-muskowitowych i muskowitowo-biotytowych, podczas gdy w łupkach gruboblastycznych (odsł. 1–9) nieregularne, wydłużone soczewki kwarcowe, z nielicznymi blaszkami muskowitu są opływanie przez smugi i laminy muskowitowo-biotytowe. Laminy lyszczykowe w obu odmianach łupków zawierają liczne porfiroblasty granatu. W łupkach gruboblastycznych osiągają one rozmiary 4–10 mm, a w łupkach drobnoblastycznych nie przekraczają 3 mm średnicy.

W okolicach Byczenia odstaniają się drobnoblastyczne łupki lyszczykowe z albitem (Fig. 2). W odróżnieniu od opisanych powyżej łupków drobnoblastycznych zawierają liczne porfiroblasty albitu (Fig. 4), natomiast brak w nich staurolitu oraz porfiroblastów andaluzytu. Łupki z albitem składają się z drobnoblastycznego tła złożonego z kwarcu, biotytu, chlorytu, muskowitu i plagioklazu oraz z soczewek i lamin kwarcowych bądź muskowitowo-biotytowych. Zarówno w tle skalnym jak i laminach lyszczykowych mogą występować nieliczne relikty granatów lub bardzo małe (poniżej 0,05 mm) blasty tego minerału.

Łupki lyszczykowe z okolic miejscowości Stolec (Fig. 3) charakteryzują się dużą zmiennością struktury i składu mineralnego. Na zachód od wspomnianej wsi (odsłonięcia 1S, 2S) występują łupki lyszczykowe o ubogim składzie mineralnym i drobnoblastycznej strukturze. Zbudowane są głównie z kwarcu, muskowitu, biotytu i plagioklazu. W niektórych partiach łupków lyszczykowych duże porfiroblasty (do 3 mm) tworzy albit. Na wschód i północ od Stolca łupki lyszczykowe mają bogatszy skład mineralny i są średnioziarniste (odsłonięcia 6S, 7S). Poza kwarcem, muskowitem, biotytom i oligoklazem, w dużej ilości występuje w nich granat, staurolit i chloryt, a w nieco mniejszej andaluzyt i sylimanit.

## METAMORFIZM

Badania Józefiaka (1994, 1996) w okolicach Kamieńca Ząbkowickiego sugerują, że na obszarze tym można wyróżnić dwie odmiany strukturalne łupków lyszczykowych: grubo- i drobnoblastyczną. Obie odmiany łupków lyszczykowych zachowały zapis odmiennych warunków metamorfizmu. Łupki gruboblastyczne osiągnęły maksimum metamorfizmu w temperaturze 570–640°C, przy ciśnieniu 8,0–13 kbar, podczas gdy łupki drobnoblastyczne zarejestrowały metamorfizm w temperaturze 510–540°C przy

ciśnieniu 7,0–8,5 kbar. Końcowy etap metamorfizmu w obu odmianach łupków reprezentuje parageneza Ms+Bt+Grt+Pl+And±Sil±St. Ciśnienia i temperatury w jego trakcie obrazują współwystępowanie andaluzytu i lokalnie następującego sylimanitu (poniżej 4 kbar i powyżej 530°C).

## STRUKTURY DEFORMACYJNE

W łupkach lyszczykowych z okolic Kamieńca Ząbkowickiego wyróżniliśmy trzy podstawowe zespoły struktur deformacyjnych odpowiadające co najmniej trzem głównym etapom deformacji D<sub>1</sub>, D<sub>2</sub> i D<sub>3</sub> o znaczeniu regionalnym. Do zespołu struktur deformacyjnych powstałych w etapie D<sub>1</sub> zaliczamy foliację S<sub>1</sub> i lineację L<sub>1</sub>. Z etapem D<sub>2</sub> wiążemy natomiast powstanie fałdów F<sub>2</sub>, kliważu krenulacyjnego i foliacji S<sub>2</sub> oraz lineacji L<sub>2</sub>. W ostatnim etapie D<sub>3</sub> rozwinięła się lineacja L<sub>3</sub> występująca na powierzchniach foliacji S<sub>3</sub> równoległych do foliacji S<sub>2</sub>.

Obserwacje strukturalne wykazały, że w okolicach Kamieńca Ząbkowickiego foliacja S<sub>1</sub> i lineacja L<sub>1</sub> są wykształcone penetratywnie w łupkach, które charakteryzują się grubym lub bardzo grubym ziarnem. Drobniejsze ziarno mają natomiast łupki, w których powierzchnie S<sub>1</sub> zostały zatarte przez młodszą, penetratywną foliację S<sub>2+3</sub>. W badanym terenie łupki gruboblastyczne występują w bezpośrednim sąsiedztwie Kamieńca Ząbkowickiego, podczas gdy łupki drobnoblastyczne odsłaniają się w okolicach Byczenia (Fig. 2). Dalej ku północy w rejonie Stolca (Fig. 3) ekwiwalentem łupków gruboblastycznych są skały występujące na wzgórzu Wałipenna i na północ od niego (Fig. 3 – odsłonięcia 3S i 6S). W pozostałych odsłonięciach położonych w pobliżu wsi Stolec dominują łupki drobnoblastyczne.

Foliację łupków gruboblastycznych (S<sub>1</sub>) wyznacza równolegle ułożenie blaszek lyszczyków oraz orientacja naprzemianległych warstewek kwarcowych i lyszczykowych. W rejonie Kamieńca Ząbkowickiego (Fig. 2) foliacja S<sub>1</sub> wykazuje zróżnicowaną orientację (Fig. 7). Najczęściej ma ona upad ku NW pod dużym lub umiarkowanym kątem (odsłonięcia 1, 2, 3), miejscami też zanurza się łagodnie ku SE (odsłonięcia 6 i 7). Zmienna orientacja foliacji jest wynikiem występowania fałdów F<sub>2</sub>, które na diagramach strukturalnych (Fig. 5) wywołują rozrzuł pomiarów powierzchni S<sub>1</sub> wzdłuż pasa o osi NE–SW. W odsłonięciach położonych blisko granicy łupków gruboblastycznych (odsłonięcia 5, 8, 9) foliacja S<sub>1</sub> ma jednolity upad ku W pod niewielkim kątem (Fig. 6). W okolicach Stolca (odsłonięcia 3S i 6S) struktury S<sub>1</sub> wykazują wyraźny rozrzuł wzdłuż pasa o osi zorientowanej NE–SW (Fig. 8). Na powierzchniach foliacji łupków gruboblastycznych lineacja intersekcjona L<sub>2</sub> zacięta starszą lineację z rozciągania L<sub>1</sub>. Ta ostatnia jest lineacją mineralną lyszczyków, którą podkreśla miejscami wydłużenie wrzecionowatych agregatów kwarcowych. Generalnie, ma ona orientację W–E lub WNW–ESE (Fig. 5, 7).

W łupkach gruboblastycznych licznie występują duże ziarna granatu. Mają one cechy synkinematycznych porfiroblastów powstały w trakcie deformacji D<sub>1</sub>. Świadczą o tym sigmoidalne smugi wrostków (Fig. 9), obecne w wielu kryształach. Porfiroblastom granatu towarzyszą cienie ciśnienia, których asymetria wskazuje na niekoaksjalne ścinanie o zwrocie "strop-ku-E" lub "strop-ku-ESE" po powierzchniach subhoryzontalnej foliacji.

Foliację S<sub>1</sub> deformują fałdy mezoskopowe F<sub>2</sub> o amplitudzie sięgającej od kilkunastu centymetrów do kilku metrów. Ich osie mają w przybliżeniu orientację NE–SW, taką jak lineacja L<sub>2</sub>, a powierzchnie osiowe zapadają łagodnie ku NW lub SE. W odsłonięciach położonych na zachód od Kamieńca Ząbkowickiego i w okolicach Stolca fałdy F<sub>2</sub> są średniopromienne. Ich dłuższe skrzydła zapadają stromo ku NW, podczas gdy krótsze skrzydła są łagodnie nachylone ku SE (Fig. 10). Fałdom F<sub>2</sub> towarzyszy kliważ krenulacyjny S<sub>2</sub> będący ich kliważem osiowym. Dwa maksima widoczne na diagramie strukturalnym (Fig. 11) pokazują zmienną

orientację kliważu na przeciwnieległych skrzydłach fałdów F<sub>2</sub>.

W badanych skałach można prześledzić kolejne etapy rozwoju powierzchni S<sub>2</sub> od kliważu krenulacyjnego po penetratywną foliację (Fig. 12). W łupkach gruboblastycznych foliacja S<sub>1</sub> pozostaje główną strukturą planarną skały. Jest ona zdeformowana przez symetryczne fałdki, których powierzchnie osiowe wyznaczają kliważ krenulacyjny. W łupkach drobnoblastycznych powierzchnie S<sub>2</sub> stanowią główną foliację tych skał, podkreślającą przez naprzemianległe warstewki lyszczykowe oraz lyszczykowo-kwarcowe. Starsza foliacja S<sub>1</sub> jest zachowana w mikrolitonach kwarcowo-lyszczykowych jako przeguby krenulacyjne (Fig. 12). W niektórych partiach łupków foliacja S<sub>2</sub> niemal całkowicie zaciera starszą foliację S<sub>1</sub>. Jej relikty spotyka się jedynie w postaci smug wrostków w porfiroblastach oraz jako przeguby fałdów śródfoliacyjnych F<sub>2</sub> (Fig. 13). Foliacja S<sub>2</sub> w łupkach drobnoblastycznych ma w badanym terenie jednolitą orientację. Wykazuje ona konsekwentnie upad ku WNW pod niewielkim kątem (Fig. 8, 14).

Przecięcie powierzchni kliważu S<sub>2</sub> z foliacją S<sub>1</sub> łupków gruboblastycznych tworzy lineację intersekcyjną L<sub>2</sub>, równoległą do przegubów fałdów F<sub>2</sub>. Jednocześnie na foliacji S<sub>2</sub> łupków drobnoblastycznych lineacja L<sub>2</sub> jest lineacją mineralną z rozciągania wyznaczoną przez równoległe ułożenie ziaren lyszczyków. Orientacja lineacji L<sub>2</sub> jest dość jednolita w skali całego obszaru. Przebiega ona NE-SW lub ENE-WSW, zanurzając się łagodnie ku SW lub WSW (Fig. 7, 8, 14).

W łupkach drobnoblastycznych występują liczne porfiroblasty granatu, z których przynajmniej część powstała w trakcie deformacji D<sub>2</sub> (Fig. 9, 15). Porfiroblastom towarzyszą dobrze wykształcone cienie ciśnienia. Ich symetryczny kształt dowodzi, że niektóre partie łupków drobnoblastycznych zarejestrowały jedynie efekty odkształcenia koaksjalnego.

Łupki drobnoblastyczne z albitem odsłonięte w okolicach Byczenia i na zachód od Stolca (Fig. 2, 3) nie różnią się pod względem strukturalnym od pozostałych łupków określanych w tej pracy jako drobnoblastyczne. Istotnie różny jest natomiast w tych skałach synkinematyczny zespół mineralny związany z etapem D<sub>2</sub>. Najważniejszym składnikiem tego zespołu są liczne porfiroblasty albitu (Fig. 4).

Przeważająca część łupków drobnoblastycznych zarejestrowała efekty niekoaksjalnego ścinania wzduż powierzchni S<sub>3</sub> równoległych do foliacji S<sub>2</sub>. Liczne wskaźniki kinematyczne (Fig. 16) dokumentują konsekwentnie zwrot ścinania "strop-ku-SW" lub "ku-WSW" po łagodnie nachylonej foliacji. Kierunek ścinania wyznacza lineacja z rozciągania L<sub>3</sub> rozwinięta na powierzchniach foliacji S<sub>2+3</sub>, równolegle do lineacji L<sub>2</sub>. Ma ona charakter lineacji mineralnej lyszczyku i zanurza się konsekwentnie ku WSW (Fig. 8, 14). Niekoaksjalne ścinanie w etapie D<sub>3</sub> przebudowuje starszą więźbę łupków drobnoblastycznych powstałą w wyniku koaksjalnego odkształcenia tych skał podczas etapu D<sub>2</sub> (Fig. 15). Generalnie udział deformacji D<sub>3</sub> w całkowitym odkształceniu łupków drobnoblastycznych, wyrażony przez rosnącą asymetrię ich więźby, zwiększa się z zachodu na wschód w kierunku granicy oddzielającej łupki z granatem i staurolitem od łupków z albitem. W tych ostatnich zaznacza się podobna tendencja – wzrost asymetrii więźby (w tym przypadku ku zachodowi) w stronę kontaktu obu odmian łupków drobnoblastycznych.

Charakterystycznym składnikiem łupków lyszczykowych są porfiroblasty andaluzytu (Fig. 17). Brak ich jedynie w łupkach drobnoblastycznych z albitem. W łupkach gruboblastycznych oraz w łupkach drobnoblastycznych o symetrycznej więźbie andaluzyt tworzy zawsze porfiroblasty postkinematyczne. Natomiast w łupkach mających więźbę asymetryczną występują synkinematyczne blasty tego minerału powstałe w trakcie deformacji D<sub>3</sub> (Fig. 17c).

## ORIENTACJA OSI <c> KWARCU

W łupkach gruboblastycznych występują trzy podstawowe rodzaje rozrzutu osi <c>: (1) wzduż pojedynczego pasa rozrzutu nachylonego do foliacji, (2) wzduż krzyżujących się pasów rozrzutu (I typ krzyżujących się pasów rozrzutu wg: Schmid & Casey, 1986) lub dwóch kół małych wokół normalnej do foliacji i (3) rozrztu izotropowy. Pojedynczy pas rozrzutu nachylony pod dużym kątem do foliacji (Fig. 18a, b) uznaje się za efekt deformacji niekoaksjalnej zbliżonej do prostego ścinania (Schmid & Casey, 1986). Nachylenie pasa rozrzutu wskazuje na ścinanie o zwrocie "strop-ku-E" charakterystyczne dla deformacji D<sub>1</sub>. Rozrzut wzduż krzyżujących się pasów (Fig. 18c, d) lub wzduż dwóch kół małych wokół normalnej do foliacji (Fig. 18e) jest rezultatem deformacji koaksjalnej (Schmid & Casey, 1986), odpowiednio, czystego ścinania i ogólnego spłaszczenia. Koaksjalną deformację łupków gruboblastycznych, zarejestrowaną przez więźbę kwarcu, należy wiązać z rozwojem kliważu krenulacyjnego w etapie D<sub>2</sub>. Izotropowy rozrzut osi <c> kwarcu na diagramach (Fig. 18f) można natomiast wyjaśniać jako rezultat statycznej rekrytalizacji kwarcu po zakończeniu podatnej deformacji.

W łupkach drobnoblastycznych (Fig. 19) stwierdziliśmy występowanie dwóch podstawowych typów rozrzutu osi <c> kwarcu: (1) wzduż pojedynczego pasa nachylonego do foliacji (Fig. 19a–d) oraz (2) wzduż krzyżujących się pasów rozrzutu (I typ krzyżujących się pasów rozrzutu) prostopadłych do foliacji (Fig. 19g–i). Pierwszy z wymienionych rodzajów rozrzutu wskazuje na deformację niekoaksjalną, zbliżoną do prostego ścinania, podczas gdy drugi jest przypuszczalnie efektem deformacji koaksjalnej o charakterze czystego ścinania (Schmid & Casey, 1986). Nachylenie pasa rozrzutu na diagramach reprezentujących deformację niekoaksjalną wskazuje konsekwentnie na ścinanie o zwrocie strop-ku-SW. W nawiązaniu do obserwacji strukturalnych, powstanie rozrzutu osi <c> kwarcu wzduż dwóch krzyżujących się pasów uznajemy za efekt deformacji D<sub>2</sub>, natomiast rozrzut wzduż pojedynczego pasa wiązemy z deformacją D<sub>3</sub>.

Rozrzuty osi <c> kwarcu uzyskane na diagramach z łupków lyszczykowych odsłoniętych w pobliżu Stolca (Fig. 20) reprezentują niemal pełną gamę przejść od pojedynczego pasa nachylonego do foliacji (Fig. 20a, b) do I typu krzyżujących się pasów (Fig. 20e). Otrzymane diagramy rozrzutu osi <c> kwarcu sugerują, że całkowite odkształcenie łupków lyszczykowych z okolic Stolca było wypadkową składowej prostego ścinania oraz składowej koaksjalnej miesiączącej się w zakresie od czystego ścinania po ogólnie spłaszczenie. Podobnie jak w okolicach Kamieńca Ząbkowickiego rozrzut osi <c> kwarcu w łupkach z otoczenia wsi Stolec interpretujemy jako efekt superpozycji deformacji D<sub>2</sub> i D<sub>3</sub>.

## DYSKUSJA

Efekty najstarszej deformacji (D<sub>1</sub>) są zachowane w łupkach gruboblastycznych. Foliacja S<sub>1</sub> stanowi tam główną powierzchnię anizotropii, podczas gdy lineacja L<sub>1</sub> została niemal całkowicie zatarta przez młodszą lineację L<sub>2</sub>. Wskaźniki kinematyczne sugerują, że foliacja S<sub>1</sub> rozwinięła się w wyniku niekoaksjalnego ścinania. Ustalenie kierunku ścinania w etapie D<sub>1</sub> utrudnia rozrzut lineacji L<sub>1</sub> na skrzydłach młodszych fałdów F<sub>2</sub> (Fig. 5). Lineacja L<sub>1</sub> miała przebieg w przybliżeniu E-W przy założeniu, że pierwotna (przed D<sub>2</sub>) orientacja foliacji S<sub>1</sub> była subhoryzontalna. W takim przypadku wskaźniki kinematyczne zarejestrowały w etapie D<sub>1</sub> ścinanie o zwrocie "strop-ku-E". Skład minerałów wyznaczających foliację S<sub>1</sub> w łupkach gruboblastycznych, a także skład występujących w nich porfiroblastów granatu sugeruje, że deformacja tych skał w etapie D<sub>1</sub> zachodziła w warunkach górnej facji amfibolitowej (Józefiak, 1996).

Foliacja S<sub>1</sub> łupków gruboblastycznych została zreorientowa-

na w etapie D<sub>2</sub> na skrzydłach fałdów F<sub>2</sub>. Północno-zachodnia asymetria wspomnianych fałdów (Fig. 10) sugeruje, że cała seria skalna odsłonięta w okolicach Kamieńca Ząbkowickiego i Stolca stanowi strome skrzydło asymetrycznego makrofału F<sub>2</sub>. Wniosek ten potwierdza orientacja kliważu krenulacyjnego S<sub>2</sub>, który na dłuższych, bardziej stromych skrzydłach fałdów F<sub>2</sub> ma nachylenie mniejsze niż foliacja. Powstaniu fałdów F<sub>2</sub> wraz z ich kliważem osiowym S<sub>2</sub> towarzyszyła koaksjalna deformacja łupków grubo-blastycznych. Lineacja L<sub>2</sub> o orientacji NE-SW lub ENE-WSW powstała w wyniku koaksjalnego rozciągania oraz z przecięcia foliacji S<sub>1</sub> i kliważu S<sub>2</sub>.

Przejście od łupków grubo- do drobnoblastycznych jest związane z przekształceniem kliważu krenulacyjnego S<sub>2</sub> w główną foliację skały. Przemiana ta nastąpiła w wyniku zróżnicowania skały na naprzemianlegle warstewki kwarcowe i łyszczkowe równolegle do kliważu S<sub>2</sub>. Przypuszczamy, że dyferencjacja łupku na warstewki o różnym składzie miała związek ze wzrostem wielkości odkształcenia w trakcie deformacji D<sub>2</sub>.

Skład minerałów wyznaczających foliację S<sub>2</sub> łupków drobnoblastycznych, a także skład powstałych równocześnie porfiroblastów granatu sugeruje, że deformacja D<sub>2</sub> zachodziła w warunkach dolnej facji amfibolitowej (Józefiak, 1996). Zonalność składu chemicznego granatu w łupkach drobnoblastycznych (z granatem i staurolitem) wskazuje na wzrost temperatury w trakcie etapu D<sub>2</sub>.

Deformacja D<sub>3</sub> była związana z niekoaksjalnym ścinaniem o zwrocie "strop-ku-WSW", które zachodziło w warunkach znacznego spadku ciśnienia. Wskazuje na to występowanie andaluzytu zarówno w grubo- jak i drobnoblastycznej odmianach łupków. Obecność tego minerału sugeruje spadek ciśnienia od 7–8 kbar w etapie D<sub>2</sub> do 2–4 kbar w etapie D<sub>3</sub> przy wciąż stosunkowo wysokiej temperaturze, przekraczającej 500°C.

Wyraźny kontrast w stopniu metamorfizmu różni łupki grubo- i drobnoblastyczne ze staurolitem i porfiroblastami granatu od łupków drobnoblastycznych z albitem. W oparciu o różnice stopnia metamorfizmu i składu litologicznego wydzieliśmy w badanym terenie dwie jednostki tektoniczne: jednostkę Kamieńca (wyższy metamorfizm) i jednostkę Byczenia (niższy metamorfizm). Granica obu wyróżnionych jednostek przebiega na zachód od Byczenia (Fig. 2) i kontynuuje się w okolicach Stolca na zachód od szczytu wzgórza Wapienna (Fig. 3).

W okolicach Stolca wychodnia łupków z albitem przebiega na zachód od wychodni łupków ze staurolitem i granatem (Fig. 3). Sytuacja taka jest wynikiem fałdowania w etapie D<sub>2</sub>. Jednocześnie w okolicach Kamieńca Ząbkowickiego i Byczenia łupki ze staurolitem i granatem odsłaniają się na zachód od łupków z albitem (Fig. 2). Takie położenie wychodni obu jednostek tektonicznych jest tam efektem przemieszczeń wzdłuż niskokątowej strefy podatnego ścinania o upadzie ku WSW i o zrzuconym skrzydle zachodnim (Fig. 21). Strefa ta jest równoległa do foliacji S<sub>2+3</sub>, która w okolicach Byczenia zapada konsekwentnie ku WSW pod kątem około 20°. Jednocześnie liczne wskaźniki kinematyczne jednoznacznie określają zrzutowo-normalny (strop-ku-WSW) zwrot ścinania w tej strefie.

Deformacja D<sub>1</sub>, której zapis zachował się w łupkach grubo-blastycznych stanowi naszym zdaniem odpowiednik deformacji opisanej jako D<sub>1</sub> (Mazur & Puziewicz, 1995b) w paragnejsach z

Chałupek (Fig. 22). W obu obszarach deformacja ta zachodziła w warunkach retrogradacji metamorfizmu od górnej do dolnej facji amfibolitowej i wiązała się przypuszczalnie ze ścinaniem o zwrocie "strop-ku-E". Koaksjalna deformacja łupków łyszczkowych znajduje natomiast swój odpowiednik w deformacji ortognejsów z Doboszowic (Fig. 22). Ortognejsy, zinterpretowane jako syntektoniczna intruzja (Mazur & Puziewicz, 1995), uległy odkształceniu o znaczącej składowej koaksjalnej. Deformacja ortognejsów w etapie D<sub>2</sub> obejmowała także składową prostego ścinania o zwrocie "strop-ku-NE" (Mazur & Puziewicz 1995b). Efekty deformacji D<sub>3</sub>, zapisanej w łupkach drobnoblastycznych, zarejestrowały także późnotektoniczne granite z Lipnik (Mazur *et al.*, 1997). Deformacja ta wiązała się w obu przypadkach z rozwojem niskokątowych, zrzutowo-normalnych stref ścinania, o zwrocie "strop-ku-WSW".

W świetle zebranych obserwacji łupki metamorfiku Kamieńca występują na krótkim skrzydle makrofału F<sub>2</sub> o stromym upadzie ku NW. Jednocześnie paragnejsy z Chałupek (Fig. 23) znajdują się na przeciwnym, dłuższym skrzydle, łagodnie nachylonym ku WNW. Oba skrzydła makrofału F<sub>2</sub> połączyć można w asymetryczną synformę obaloną ku SE, której oś przebiega NE-SW.

Rekonstrukcja makrosyntez F<sub>2</sub> pozwala na ustalenie wzajemnego położenia trzech dużych jednostek tektonicznych występujących w badanym terenie. Od góry do dołu są to: (1) jednostka Chałupek (paragnejsy i amfibolity), (2) jednostka Kamieńca oraz (3) jednostka Byczenia. Jednostki te reprezentują naszym zdaniem trzy płaszczyzny, które przed etapem D<sub>2</sub> zalegały płasko na sobie. Sekwencja wyróżnionych jednostek wykazuje, typową dla budowy płaszczyznowej, tektoniczną inwersję stopnia metamorfizmu. Dwie górne płaszczyzny (Chałupek i Kamieńca) mają wyższy stopień metamorfizmu (góra facja amfibolitowa) od płaszczyzny Byczenia (dolina facja amfibolitowa lub pogranicze facji zieleńcowej i amfibolitowej) położonej najniżej. Jednostki Chałupek i Kamieńca różni natomiast od siebie maksymalny zakres temperatury, jaki zapisał się w nich podczas wczesnych faz metamorfizmu. Najwyższa położona jednostka Chałupek zawiera soczewki granulitów zmetamorfizowanych w temperaturze do 920°C (Achramowicz *et al.*, 1995), podczas gdy w niżejlegiej jednostce Kamieńca występują eklogity rejestrujące temperaturę 575°C (Achramowicz *et al.*, 1997).

## PODSUMOWANIE I WNIOSKI

Serie skalne odsłonięte pomiędzy blokiem sowiogórskim a masywem Niedźwiedzia wykazują budowę płaszczyznową. Trzy jednostki tektoniczne (Chałupek, Kamieńca i Byczenia) o odrebrnej historii metamorfizmu są nasunięte na siebie ku wschodowi w rezultacie deformacji D<sub>1</sub>. Lineacja o przebiegu NE-SW, dominująca w badanym terenie, jest efektem fałdowania i koaksjalnej kontrakcji wzdłuż kierunku NW-SE, podczas deformacji D<sub>2</sub>. Kliważ osiowy fałdów F<sub>2</sub> rozwinał się miejscami w penetratywną foliację S<sub>2</sub> zacierającą starszą foliację S<sub>1</sub>. Deformacji D<sub>2</sub> towarzyszyła przypuszczalna syntektoniczna intruzja przekształcona w ortognejsy z Doboszowic. Ewolucję obszaru zakończył kolaps ekstensyjny ku WSW, związany z rozwojem niskokątowych, zrzutowo-normalnych stref podatnego ścinania.